NACA RM E56C07

NACA

RESEARCH MEMORANDUM

EXPERIMENTAL AND ANALYTICAL INVESTIGATION OF AN ACCELERATION REGULATING CONTROL FOR A TURBOJET ENGINE

By Paul M. Stiglic, Herbert Heppler, and David Novik

Lewis Flight Propulsion Laboratory
Cleveland, Ohio

NATIONAL ADVISORY COMMITTEE FOR AERONAUTICS

WASHINGTON

June 28, 1956

Declassified October 28, 1960

NACA RM E56C07

NATIONAL ADVISORY COMMITTEE FOR AERONAUTICS

RESEARCH MEMORANDUM

EXPERIMENTAL AND ANALYTICAL INVESTIGATION OF AN ACCELERATION REGULATING CONTROL FOR A TURBOJET ENGINE

By Paul M. Stiglic, Herbert Heppler, and David Novik

SUMMARY

An acceleration control that operates on fuel flow and uses directly measured acceleration as the control signal was applied to an axial-flow turbojet engine. This control limited and regulated acceleration in accordance to a preset schedule. A study to determine the feasibility and dynamic characteristics of this control was undertaken.

Three types of control action, integral, proportional-plus-integral, and proportional, were used and studied. Open- and closed-loop studies of each control system were made to determine stability, droop, and overshoot characteristics. The effect of the noisy acceleration signal on the controls operation was studied.

The control operated quite well with integral and proportional-plus-integral control actions and operated unsatisfactory with proportional actions.

With the use of integral or proportional-plus-integral control actions, the control limited and regulated acceleration. These control actions were not hampered by the noisy acceleration signal and each showed identical droops that could be accurately predicted and did not seriously affect the control accuracy. However, the proportional-plus-integral control action showed a smaller overshoot and an ability to remain stable at higher loop gains than did the integral action.

With proportional control action, the control acted as an acceleration limiter only, showed undesirable droop characteristics, and was seriously hampered by the noisy acceleration signal.

INTRODUCTION

In order to change thrust level quickly, by means of speed, a turbojet engine must be accelerated from one rotor speed to another in the

shortest time possible. Previous investigations have shown the region of maximum rotor acceleration to be located on the stall line throughout the operating range (ref. 1). The problem with respect to control design is accelerating the engine at the maximum rate without encountering surge, stall, or overtemperature. This can be done in two general ways:

(1) Schedules that limit engine variables such as fuel flow, acceleration, compressor discharge pressure, or temperature

(2) Optimalizing techniques that require some signal from the engine to warn of impending stall or surge

Although the optimalizer technique may not require altitude or engine deterioration correction and could utilize maximum engine acceleration potential, no usable signal for its operation has yet been established (ref. 2).

The purpose of this investigation is to study the dynamic characteristics and operating problems associated with a schedule-type control using directly measured acceleration as the control signal. An advantage of an acceleration control over most of those using other engine parameters is the large margin that exists between the steady-state acceleration (zero) and the maximum value at the stall line. This margin represents the safe operating region of the engine.

A plot of the margin of a particular turbojet compressor-discharge pressure against speed is presented in figure 1(a). Data for this plot were obtained from reference 3. The margin is less than 1 pound per square inch at speeds below 48 percent and less than 3 pounds per square inch at all speeds below 65 percent rated. Within this small margin, allowance must be made for engine deterioration, production deviation, inlet distortion, and sensing instrumentation errors. The margin shown in figure 1(a) would be difficult to work with because it is such a small percentage of the pressure being sensed. For example, if the sensing instrument were accurate to within 1 percent, the margin at 60 percent speed would have to be reduced 15 percent to compensate for this error. Allowance for these various factors can limit the already small margin and seriously hamper the effectiveness of the control.

Control schemes using tailpipe or turbine-inlet temperature are also hampered by a narrow operating margin. In addition, a temperature control must somehow compensate for the thermocouple dynamics that would complicate the control and reduce its reliability. Problems of temperature controls are discussed in reference 4.

The variation of acceleration margin with speed of the same engine is shown in figure 1(b). Data for this plot was taken from reference 1. From figure 1(b), the margin is never less than 300 revolutions per minute per second over the range shown. An error of 1 percent in the sensing instrumentation would make it necessary to reduce the margin only 1 percent to compensate for this error. Allowances for all other corrections necessary in the pressure schedule of figure 1(a) would also have to be made with the acceleration schedule; but, with such a large margin available and with less of the margin consumed with sensing instrumentation errors, more of the accelerating potential of the engine could be utilized.

Since the purpose of this investigation was to study dynamic characteristics and operating problems of the acceleration control, an optimum schedule, such as the one shown in figure 1(b), was not incorporated in the control. For simplicity, a schedule that was constant with speed was used. Also for simplicity, no provision was made to prevent overtemperature operation.

The basic difficulty of using acceleration in the past has been its measurement. A speed sensor is used and its output differentiated. Differentiation has the undesirable characteristic of amplifying high frequency components of an incoming signal and greatly reducing the output signal to noise ratio. This noise can be eliminated by filtering the output, but the dynamics of these filters appear as lags in the control loop. These lags can affect the accuracy and stability of the control. During this investigation, filtering was held to a minimum and the effectiveness of the control operating with some noise still on the signal was observed.

SYMBOLS

The following symbols are used in this report:

a	dead time, sec
C	capacitive component
C_1	rate of input signal ramp, v/sec
C_2	magnitude of desired setting, v
E	voltage, v
G_l	loop gain of control
j	imaginary number

K_b transfer function of speed measuring system, v/rpm

K_c gain of the control-action circuit

K_e steady-state engine gain of speed to fuel flow at constant area, rpm/lb/hr

K_f transfer function of fuel valve, v/lb/hr

K_p proportional gain

$\frac{K_1}{P_2}$ gain of $\dot{N}_m$ signal through subtractor network where $K_1 = R_7/R_6$

$\frac{K_2}{P_2}$ gain of $\dot{N}_s$ signal through subtractor network where $K_2 = R_7/R_5$

N engine speed, rpm

$\dot{N}$ acceleration, rpm/sec

P potentiometer setting

R resistive component, ohms

s Laplacian operator

t time, sec

w_f fuel flow, lb/sec

τ_d time constant of differentiator, sec

τ_e engine time constant, sec

τ_f time constant of filter, sec

τ_i time constant of integrator, sec

τ_s time constant of stabilizing lag in derivative circuit, sec

ω frequency, cps

Subscripts:

m	measured
s	set
1,2,3 . . .	designation of resistor, potentiometer, or capacitor from figure 6

DESCRIPTION OF CONTROL SYSTEM

A block diagram of the control loop is shown in figure 2. Adder, filter, derivative network, subtractor, acceleration schedule, control action, and ramp generator circuits were set up on an electronic computer and wired into their proper positions in the loop.

The level setting shown at the adder of figure 2 is a part of the fuel-valve servo and is used to set the initial steady-state speed. The throttle is simply a switch which, when closed, sends a step-shaped signal to the ramp generator. The ramp generator converts the step to a ramp that limits at some preset value. The ramp effects an increase in fuel flow which causes the engine to accelerate to some new steady-state speed.

Basically, the control will start to operate only after the scheduled acceleration has been exceeded. A diode switch maintains the control inoperative until the error signal becomes positive, indicating the scheduled acceleration has been exceeded. The control action then sends a negative signal to the adder which reduces fuel flow and, consequently, the measured acceleration $\dot{N}_m$. The control remains in operation until the output of the control action circuit returns to zero, at which point the diode switch again renders it inoperative.

Three basic types of control action, integral, proportional, and proportional-plus-integral, were used in the investigation.

With integral control action $1/\tau_i s$, the control acted like a combination limiter and regulator. It was a limiter because the diode would not allow it to operate until the scheduled acceleration was first reached and was a regulator because it attempted to maintain acceleration at a set value for a period of time. The regulating action comes about because the output of the control action is the integral of the error with respect to time and the control remains in action until this output reaches zero. When the desired acceleration is exceeded, the output of the control action becomes increasingly negative, which will

subtract fuel and reduce acceleration. When the error then goes negative ($\dot{N}_m$ too small), the output of the control action becomes less negative, which effectively increases fuel flow and increases acceleration. The time constant of the integral control action τ_i was set at 0.25 second for the entire program.

With proportional-plus-integral control action $K_p + \frac{1}{\tau_i s}$, the control was again a limiter-regulator combination and its basic operation was exactly the same as for integral control action.

With proportional control action K_p, the control was a limiter only. When the error goes to zero at anytime, the control-action output goes to zero and is switched out of action because the output of the control action (fig. 2) is now simply a constant times the input. This means that control action will be maintained only when $\dot{N}_m$ is greater than the set acceleration $\dot{N}_s$.

Fuel System

The fuel system is shown in figure 3. The fuel valve used was a reducing-type differential-pressure regulator which maintained a constant pressure drop across the throttle. The throttle is actuated by an electro-hydraulic servomotor. Response of the throttle to an input signal is essentially flat to 20 cycles per second and, with the amplifier-gain setting used, resonated at about 60 cycles per second (ref. 5). For analytical purposes the fuel-valve transfer function was taken as a constant and designated K_f.

Engine

The engine selected for the investigation was an axial-flow turbojet. The response of speed to fuel of a turbojet engine within its linear operating range is a first order lag and is written as

$$\frac{\Delta N}{\Delta w_f} = \frac{K_e}{1 + \tau_e s}$$

In addition, a dead time has been found to exist between fuel flow and speed in a turbojet engine. This dead time is thought to be composed of transport time required by the fuel system and combustion lags. Figure 4 illustrates this dead time of the engine tested at two engine speeds. In figure 4(a), the engine is subject to step input in fuel flow as indicated by the fuel-valve position trace, but engine speed

does not respond until 0.040 second later. In figure 4(b), which was run at a lower engine speed and used a smaller step, a 0.040-second dead time is again detectable. In order to properly account for this dead time, the transfer function of speed to fuel flow is written as

$$\frac{\Delta N}{\Delta w_f} = \frac{K_e}{1 + \tau_e s} e^{-ja\omega} \tag{1}$$

where a is the dead time.

Engine characteristics pertinent to equation (1) are presented in figure 5. Figures 5(a) and (b) are the speed to fuel flow gain and engine time constant plots, both plotted against engine speed. Figure 5(c) is the ratio of engine gain to engine time constant, also plotted against speed. The significance of figure 5(c) is that the amplitude response of speed to fuel flow at all frequencies higher than the break frequency, determined by τ_e, is a function of the ratio of engine gain to time constant. Figure 5(c) shows a peak at about 75 percent rated engine speed, at which point a control for speed or acceleration on this engine would be most likely to become unstable.

The engine utilized a flow divider combined with large- and small-slot manifolds in its fuel system. Difficulty was encountered with this system in that the large-slot manifold would drain when not in use and would have to be filled before supplying fuel to the engine. At the point where the manifold is filled, the engine receives a sudden increase in fuel and an overshoot in acceleration results.

Speed Measuring Circuit

A tachometer - pulse-counter combination was used that produced a direct-current voltage proportional to engine speed. The manufacturer's manual gives a response time of 1 millisecond which, if thought of as the first order time constant of the system, yields a frequency response flat to 160 cycles per second. For analytical purposes its transfer function was taken as the constant K_b.

Differentiator

The differentiator circuit was set up on the computer and its transfer function is $\frac{\tau_d s}{1 + \tau_s s}$. The lag in the denominator is necessary to stabilize the computer amplifier and was made very small ($\tau_s = 0.015$ sec).

Filter

The filter was a first order lag $\frac{1}{1 + \tau_f s}$. The value for τ_f was set at 0.10 second for all the control actions and was held constant during the entire investigation.

A circuit diagram of the control loop is shown in figure 6. The circuits for the fuel valve and speed sensing have been omitted for simplicity. The control action shown is proportional-plus-integral. Integral control action was obtained by short circuiting resistor R_{10}, proportional action by short circuiting capacitor C_3. The acceleration schedule $\dot{N}_s$ is varied by potentiometer P_1, whereas loop gain is set by P_2.

Loop gain is the product of all the terms in the open-loop transfer function that are independent of frequency. The loop gains for the controls used in this investigation were derived as follows:

Referring to figure 6,

$$\begin{pmatrix}\text{Open-loop} \\ \text{response}\end{pmatrix} = K_b K_f \left(\frac{K_e}{1 + \tau_e s}\right)\left(\frac{R_2/R_1}{1 + R_2 C_1 s}\right)\left(\frac{R_4 C_2 s}{1 + R_3 C_2 s}\right)\left(\frac{R_7}{R_6 P_2}\right)\begin{pmatrix}\text{Control} \\ \text{action}\end{pmatrix} \quad (2)$$

Assuming a sine wave input, and letting

$$R_2/R_1 = 1$$

$$R_2 C_1 = \tau_f$$

$$R_4 C_2 = \tau_d$$

$$R_3 C_2 = \tau_s$$

$$R_7/R_6 = K_1$$

equation (2) can be rewritten as

$$\begin{pmatrix}\text{Open-loop} \\ \text{response}\end{pmatrix} = K_f K_b K_c \left(\frac{K_e}{1 + \tau_e j\omega}\right)\left(\frac{1}{1 + \tau_f j\omega}\right)\left(\frac{\tau_d}{1 + \tau_s j\omega}\right)\left(\frac{K_1}{P_2}\right) \quad (3)$$

Analytical expressions for loop gain for various control schemes can now be obtained. Using integral control action $\tau_i = R_8C_3$ equation (3) can be written as

$$\text{Open-loop response} = \left(\frac{K_f K_e K_b \tau_d K_1}{\tau_i P_2}\right)\left[\frac{j\omega}{j\omega(1 + \tau_e j\omega)(1 + \tau_f j\omega)(1 + \tau_s j\omega)}\right] \quad (4)$$

where $\frac{K_f K_e K_b \tau_d K_1}{\tau_i P_2}$ is the expression for loop gain. The response of the open loop at zero frequency will be equal to the loop gain using integral control action.

If the control is made proportional-plus-integral, the control-action transfer function is $\frac{1 + K_p \tau_i j\omega}{\tau_i j\omega}$ where $K_p = R_{10}/R_8$ and the open loop response is

$$\text{Open-loop response} = \left(\frac{K_f K_e K_b \tau_d K_1}{\tau_i P_2}\right)\left[\frac{j\omega(1 + \tau_i K_p j\omega)}{j\omega(1 + \tau_e j\omega)(1 + \tau_f j\omega)(1 + \tau_s j\omega)}\right] \quad (5)$$

where the first term is again the loop gain and is the same as for the integral control.

If the control is made proportional only, equation (3) can be written as:

$$\text{Open-loop response} = \left(\frac{K_f K_e K_b \tau_d K_1 K_p}{P_2}\right)\left[\frac{j\omega}{(1 + \tau_e j\omega)(1 + \tau_f j\omega)(1 + \tau_s j\omega)}\right] \quad (6)$$

where the first term is again the loop gain. Here the open-loop response at zero frequency is zero.

The engine gain K_e varies a great deal with speed (fig. 5(a)). Since the loop gain expressions contain only two variables, K_e and P_2, loop gain will vary with speed in the same manner as the engine gain in figure 5(a) at any constant P_2 setting. Figure 7 is a plot for proportional-plus-integral and integral control actions showing loop gain as a function of speed and P_2 setting. The effect of the change of loop gain with engine speed on the control systems will be discussed in RESULTS AND DISCUSSION.

TEST PROCEDURE

All test runs were begun at 63 percent rated speed with the control inoperative. The initial speed was determined by the level setting (fig. 6). Before the initiation of a transient, the desired $\dot{N}_s$ was obtained by setting potentiometer P_1, and the loop gain was obtained by setting potentiometer P_2 (fig. 6). The switch in the throttle circuit (fig. 6) was then closed which caused a ramp increase to be imposed at the adder circuit. The output of the ramp generator continued to increase until its value was equal to battery voltage E_2 (fig. 6). The signal from the ramp generator then remained at a constant voltage E_2. The sum of the ramp generator output and level setting voltage was just enough to increase the fuel flow to rated value. The slope of the ramp was varied by potentiometer P_3. Input signal, control-action output, fuel-valve position, engine speed, and engine acceleration were recorded.

RESULTS AND DISCUSSION

Open-Loop Characteristics

The open-loop characteristics of a control are important in that the magnitude of the response at the 180° phase shift point indicates the stability of the system and the magnitude of the response at zero frequency determines the ability of the control to eliminate steady-state errors or droops. In order to evaluate these characteristics, the control loop was opened at point A (fig. 2) and a frequency response was run on the system. A sine wave input signal was compared with the control action output.

The open loop responses of the various schemes used are shown in figure 8. No experimental data was used for figure 8, which was drawn using the straight line approximations of equations (4) to (6), loop gain values from figure 7, and engine time constants from figure 5(b). The purpose of this plot is to illustrate the open-loop characteristics over a wide range of frequencies. The frequency band used in the experimental frequency response is shown by the dotted lines on figure 8. The conditions of a P_2 of 0.4, K_p of 0.4, and τ_i of 0.25 were used in plotting figure 8.

As shown in figure 8, integral and proportional-plus-integral control actions show identical responses to 1.6 cycles per second. At 1.6 cycles per second, the filter began to attenuate the integral control, while the lead term of the proportional-plus-integral control action cancelled the filter dynamics. These dynamics will cancel only when

$\tau_i K_p$ and τ_f are equal in equation (5). At 63 percent rated speed, the response of both controls are flat to 0.0091 cycle per second where the break caused by the engine time constant occurs. At 0.25 cycle per second, the response has been reduced by a factor of 25. The open-loop characteristics of the integral and the proportional-plus-integral controls are generally desirable in that the response is quite large at zero frequency and the attenuation at higher frequencies aids stability.

Amplitude response of integral and proportional-plus-integral controls at 75 percent rated speed is also plotted on figure 8 to illustrate how the peak in figure 5(c) could create a stability problem. The response at 75 percent rated speed is greater than it was at 63 percent rated speed for all frequencies above 0.02 cycle per second. If 180° phase shift occurred at, say, 1.5 cycles per second at both speeds, then figure 8 indicates the control would be stable at 63 percent rated speed and unstable at 75 percent speed.

The response of proportional control action for 63 percent rated speed is also shown in figure 8. The open-loop characteristics of this control are undesirable in that the response at zero frequency is zero and the response at higher frequencies does not attenuate nearly as well as the proportional-plus-integral or integral control actions. This poor attenuation in conjunction with the dead time of the engine creates a stability problem.

Nyquist plots of the data taken from the experimental frequency response are presented in figure 9. Figure 9(a) is the Nyquist plot for integral control action taken at 63 percent rated speed. The 180° phase shift point is reached at about 1.5 cycles per second and the control is stable. In figure 9(b), a Nyquist plot is presented for a proportional-plus-integral control action, with a K_p of 0.4 also at 63 percent rated speed. Here the 180° phase shift point is not reached until about 3.5 cycles per second which gives figure 9(b) a greater phase margin than figure 9(a). Hence, adding proportional gain to the integral control apparently improves its stability.

It is interesting to note the effect of the dead time on the Nyquist plots of figure 9. In figure 9(a), 22° of the 180° phase shift at 1.5 cycles per second is due to the dead time, whereas in figure 9(b), 53° of the 180° at 3.5 cycles per second are from this source. If this dead time were not present, higher values of loop gain could be used without encountering instability.

Closed-Loop Characteristics

Stability. - The control loop was closed and the stability characteristics of various control actions were investigated. Control actions were set up and loop gain was increased on succeeding runs until the stability limit was reached. The dotted line in figure 10 represents the stability limit evaluated in this fashion. Points from integral control action are along the abscissa, those for proportional action along the ordinate and all points for proportional-plus-integral combinations lie in between.

In order to more clearly define its shape, the stability limit was also evaluated analytically. This limit is shown as the solid line on figure 10. The stability limit was calculated by assuming a control combination and solving for the frequency that would produce 180° phase shift in the open loop. Using this frequency, the value of P_2 was established that would produce a gain of unity in the open loop. Gains and time constants for this analysis were taken at 75 percent rated speed.

The bend in the stability limit as it nears the abscissa is significant in figure 10. This would indicate that an integral control, unstable by itself, could be stabilized by the addition of the proper amount of effective proportional gain. Some experimental runs are shown to illustrate this point.

A transient using integral-control action with a τ_i of 0.25 second and a P_2 setting of 0.22 is shown in figure 11(a). This would put this run at 18.2 on the abscissa in figure 10 and beyond the stability limit. As can be seen from figure 11(a), the control is unstable. The oscillations are dampened at about the 3-second mark because of large-slot dynamics, but begin again after the 5.0-second point where the large-slot manifold has filled.

A transient of a control where the effective integral gain has been increased to 20 and to which a proportional gain of 2.0 has been added is shown in figure 11(b). This combination is near the stability limit as shown on figure 10, and the oscillations are far smaller and more confined than those of the integral action on figure 11(a). If the proportional gain of figure 11(b) were reduced to about 1.5, the oscillations should disappear entirely.

The stability limit of proportional control action was difficult to evaluate experimentally because of the limiting of the fuel valve. The run shown in figure 12 represents a proportional control action with an effective proportional gain of 7.5, which is well beyond the

limit shown on figure 10. The initial part of the $\dot{N}$ trace in figure 12 from 0 to about 3.5 seconds appears to be stable because the fuel valve is striking its lower limit and dampening the oscillations. This problem was not encountered with the integral or proportional-plus-integral actions because less 60-cycle noise was passed by the control. The proportional control action was the only control action tested that was so hampered by the noise problem.

Droop and overshoot. - An oscillograph recording of a controlled engine transient using integral control action is shown in figure 13. The transient is initiated by a ramp input signal of 2-second duration which increases fuel flow and causes the engine to accelerate. When the acceleration reaches the scheduled value, at about the 0.4-second point, the control is switched in and begins to subtract fuel. In figure 13, however, the control cannot subtract fuel quickly enough and acceleration overshoots its desired value (0.5-second point). After a few oscillations, acceleration settles to a steady value that is above the desired level. This error, which lies between the 1.0- and 2.0-second points on figure 13, is caused by the control not subtracting fuel fast enough to contend with the ramp input signal. This error will be referred to as droop A.

After the ramp input signal has reached the preset limit, the control must now add fuel to maintain the desired acceleration. The constant error that occurs between 3.4 and 4.6 seconds on figure 13 occurs because the control cannot add fuel quickly enough to maintain desired acceleration level. This error will be referred to as droop B. At the 5.2-second point, the large-slot manifold of the fuel system begins to supply fuel and a large overshoot occurs. The control then subtracts fuel in an attempt to correct this overshoot. After the large-slot overshoot takes place, acceleration again falls and the control now adds fuel to maintain desired level. Another error occurs around 7.0 seconds. This error, which is below the desired level, will be called droop C. When the control output reaches zero (8.1 seconds), the control is switched out and the engine returns to steady-state operation.

High-frequency noise from the acceleration trace is filtered by the integral control and does not appear on the control-output or fuel-valve position traces. The fuel-valve position trace, which is indicative of fuel flow, is the algebraic sum of the input-signal and control-output traces.

An uncontrolled transient is shown in figure 14(a). With a 2-second ramp input signal, the acceleration increased to nearly twice the value that was later used as a schedule, and two cycles of surge were encountered when the large-slot manifold began supplying fuel. Fuel flow had to be cut back when the surge was encountered making the acceleration unsuccessful.

A controlled transient operated with integral control action is presented in figure 14(b). The initial overshoot was held to about 61 percent over set value. It is apparent that the acceleration is now maintained much closer to the set value than it was in figure 14(a) without the control and no surge was encountered.

A transient using proportional-plus-integral control action is shown in figure 14(c). Initial overshoot has almost disappeared, the set level is maintained still more closely and the large-slot overshoot has been greatly reduced. However, the proportional part of the control action passes high frequencies and the noise from the acceleration now appears on the control-output and fuel-valve position traces. Note that the amplitude level of the noise on the fuel-valve position trace is larger than that on the control-output trace. This is because the noise frequency (60 cps) corresponds to the resonant point of the fuel valve (ref. 5).

Figure 14(d) represents a controlled run using pure proportional action. Here again, the noise appears on the control-output and fuel-valve position traces. In this control scheme, no initial overshoot is encountered, but the acceleration is not maintained as close to the desired level as in the previous schemes.

Droop: The nature of the droops encountered in the controlled transients is shown in figures 13 and 14. These droops were investigated analytically and then experimental data were compared with the analytical findings.

Equations describing droops A, B, and C using proportional-plus-integral control action are derived in the appendix and are as follows:

$$\text{Droop A} = \frac{G_l \tau_i C_1 - \frac{K_2}{P_2} C_2}{1 + G_l} \tag{A4}$$

$$\text{Droops B and C} = \frac{-\frac{K_2}{P_2} C_2}{1 + G_l} \tag{A5}$$

Proportional gain K_p of the proportional-plus-integral control does not appear in equations (A4) and (A5) and loop gain G_l, given in figure 7, has been shown to be the same for integral and proportional control actions. Therefore, droop equations (A4) and (A5) hold for integral as well as proportional-plus-integral control actions. This means that both controls operating at the same speed with the same integrator time constant and the same P_2 setting will have identical droop characteristics.

A plot of experimental data taken by starting with integral control action and adding proportional gain is presented in figure 15. Data points for droop A were taken at one constant speed, those for droop C at another. Here, droops A and C can be seen to be identical for the integral control and various proportional-plus-integral combinations tested. Droop B was not plotted, as large-slot dynamics interfered with its evaluation.

Equations (A4) and (A5) indicate that the magnitude and direction of droop A is dependent on the rate of the input-signal term C_1, whereas droops B and C are independent of this term. Figure 16 shows that droop C remains constant with changes in ramp input signal rate, whereas droop A varies greatly. In a practical control system, droop A can be limited by limiting the rate at which the input signal is applied.

Droops A, B, and C were calculated from equations (A4) and (A5) and compared with experimental values in figure 17. This plot, where droop is presented against loop gain, again holds for integral or proportional-plus-integral actions. Each droop was again evaluated at a constant speed so that loop gain varies with P_2 setting only. Figure 17 indicates close correlation between calculated and experimental results for droops A and C and also shows the effect of loop gain on droop. Poor correlation occurs for droop B because the large-slot manifold begins filling at this point which diverts fuel from the engine and reduces acceleration. How much fuel goes to filling the manifold was not known and could not be considered in the calculations. These large-slot dynamics are not generally encountered on turbojets.

From figure 17 it can be concluded that in general, droop can be accurately predicted and can also be reduced by increasing loop gain in proportional-plus-integral and integral systems.

Droop characteristics of proportional control action were impossible to evaluate experimentally. Substituting values in equation (A7) of the appendix would indicate droop A for proportional control action to be extremely large, about 7000 revolutions per minute per second for the conditions of figure 14(d). Acceleration in figure 14(d) is still increasing when the ramp input signal reaches its limit, making it impossible to evaluate droop A. Droop A is the most important of the droops since it is in the direction of an overshoot. The large droop A shown by the proportional control would make it unsatisfactory for an acceleration control.

Droops B and C for proportional control action are meaningless. Both of these droops are in the direction of an undershoot and the proportional control action being a limiter only is switched out when engine acceleration is below the scheduled value.

Overshoot: It is desirable to hold the overshoot of acceleration to a minimum on this schedule-type controller. If a significant overshoot persists in the system, the schedule would have to be shifted away from the surge line which would reduce the effectivenss of the control.

As shown on figure 13, two overshoots were encountered on each transient, one where the control first begins its action and another where the large-slot manifold begins to supply fuel. An analysis of overshoot with this particular system would prove quite difficult because of the initial conditions present when the control is switched into operation. All data to be presented here is, therefore, experimental. Control parameters were varied and their effect on overshoot noted.

A plot was made to show the effect of increasing loop gain on the initial overshoot for an integral and a proportional-plus-integral combination ($K_p = 1.0$). Figure 18 indicates that an increase in loop gain from 40 to 190 reduced the initial overshoot of the integral control action about 20 percent, and about 30 percent for the proportional-plus-integral. Also, from figure 18, the proportional-plus-integral control shows about 20 percent less overshoot at all loop gains than the integral control.

Loop gain of the same integral and proportional-plus-integral actions was then held constant and the effect of the rate of ramp input signal on initial overshoot was studied. The overshoot increases when faster ramps are used as shown in figure 19. Here again, a practical control system must limit the rate of input signal. On figure 19, the proportional-plus-integral control again shows less initial overshoot than the integral control.

Overshoot caused by large-slot dynamics was quite clear from the data and could be accurately evaluated. A clearer picture of the effect of control parameters on overshoot may be had here because the control has already been switched into operation when the large-slot overshoot occurs, thus eliminating the effect of any switching dynamics or initial conditions.

The effect of increasing proportional gain with proportional-plus-integral and proportional control actions on large-slot overshoot is shown in figure 20. Starting with integral control action, the large-slot overshoot was reduced about 29 percent by the addition of 1.4 proportional gain as indicated by the top curve on figure 20.

Proportional action showed a greater reduction by lowering the overshoot 42 percent for an increase in proportional gain from 0.1 to 1.3.

The overshoot characteristics of proportional action are the most desirable in that no initial overshoot was noted, whereas large-slot overshoot could be substantially reduced. Integral control action showed the least desirable overshoot characteristics.

CONCLUSIONS

An investigation was made to study the dynamic characteristics and operating problems associated with a schedule-type control using directly measured acceleration as the control signal.

The control scheme investigated operated quite well when integral or proportional-plus-integral control actions were used and was unsatisfactory for proportional control action.

With integral or proportional-plus-integral control actions the control limited and regulated acceleration. Noise from the acceleration signal was filtered by the integral control action and did not interfere with either the integral or proportional-plus-integral schemes. Both controls showed identical droop characteristics that would not seriously affect the accuracy of the controls and could be accurately predicted. The proportional-plus-integral control, however, showed less overshoot and showed the ability to remain stable at higher loop gains than the integral scheme, when the proper control gains were utilized.

With proportional control action, the control acted only as a limiter. Noise from the acceleration signal interfered with the operation of the fuel valve, and the control scheme showed poor droop characteristics.

A practical control could be made from this scheme that would use proportional-plus-integral control action, an acceleration schedule that varies properly with speed, and a limiter to limit the rate at which the input signal could be applied. A temperature override may also be necessary.

Lewis Flight Propulsion Laboratory
National Advisory Committee for Aeronautics
Cleveland, Ohio, March 29, 1956

APPENDIX - EQUATIONS OF DROOP

Referring to figure 2 and using the appropriate transfer functions, the closed-loop error response is a function of both input signal and $\dot{N}_s$ inputs and can be written as,

$$\text{Error} = \frac{\left(\frac{K_1\tau_d K_b K_e K_f}{P_2}\right)\left[\frac{s}{(1+\tau_s s)(1+\tau_f s)(1+\tau_e s)}\right]\left(\begin{matrix}\text{Input}\\ \text{signal}\end{matrix}\right) - \frac{K_2}{P_2}\dot{N}_s}{1 + \left(\frac{K_f K_e K_b \tau_d K_1}{P_2}\right)\left[\frac{s}{(1+\tau_e s)(1+\tau_f s)(1+\tau_s s)}\right]K_c} \tag{A1}$$

Assuming proportional-plus-integral control action, a ramp input signal of $C_1 t$ and a step of C_2 for $\dot{N}_s$, equation (A1) can be rewritten as

$$\text{Error} = \frac{\left(\frac{K_1\tau_d K_b K_e K_f}{P_2}\right)\left[\frac{s}{(1+\tau_s s)(1+\tau_f s)(1+\tau_e s)}\right]\left(\frac{C_1}{s^2}\right) - \left(\frac{K_2}{P_2}\right)\left(\frac{C_2}{s}\right)}{1 + \left(\frac{K_f K_e K_b \tau_d K_1}{P_2}\right)\left[\frac{s}{(1+\tau_e s)(1+\tau_f s)(1+\tau_s s)}\right]\left(\frac{(1+\tau_i K_p s)}{\tau_i s}\right)} \tag{A2}$$

Droop A occurs while the ramp input signal is being imposed and after initial transients have subsided. The final value of equation (A2) therefore defines droop A. In order to find this expression, equation (A2) is multiplied by s, and then s is allowed to approach zero.

$$\text{Droop A} = \frac{\frac{K_1\tau_d K_b K_e K_f C_1}{P_2} - \frac{K_2 C_2}{P_2}}{1 + \frac{K_f K_e K_b \tau_d K_1}{P_2 \tau_i}} \tag{A3}$$

Substituting the expression for loop gain of proportional-plus-integral control action from equation (4) into equation (A3) yields

$$\text{Droop A} = \frac{G_l C_1 \tau_i - \frac{K_2 C_2}{P_2}}{1 + G_l} \tag{A4}$$

Droop B occurs after the ramp input signal has reached its preset limit. Under this condition, the input signal can be thought of as a step. The effects of a step in input signal will disappear in the final value.

$$\text{Droop B} = \frac{-\frac{K_2C_2}{P_2}}{1 + G_l} \tag{A5}$$

Droop C is also described by equation (A5) and will differ only in the value of the loop gain term.

Since the proportional gain K_p does not appear in equations (A4) and (A5), these expressions also hold for integral control action.

If the control is taken as pure proportional, equation (A2) can be written as

$$\text{Error} = \frac{\left(\frac{K_1\tau_dK_bK_eK_f}{P_2}\right)\left[\frac{s}{(1 + \tau_s s)(1 + \tau_f s)(1 + \tau_e s)}\right]\frac{C_1}{s^2} - \left(\frac{K_2}{P_2}\right)\left(\frac{C_2}{s}\right)}{1 + \left(\frac{K_fK_eK_b\tau_dK_1}{P_2}\right)\left[\frac{s}{(1 + \tau_e s)(1 + \tau_f s)(1 + \tau_s s)}\right]K_p} \tag{A6}$$

The final value of equation (A6) will be droop A and is written as

$$\text{Droop A} = \frac{K_1\tau_dK_bK_eK_fC_1}{P_2} - \frac{K_2C_2}{P_2} \tag{A7}$$

REFERENCES

1. Stiglic, Paul M., Schmidt, Ross D., and Delio, Gene J.: Experimental Investigation of Acceleration Characteristics of a Turbojet Engine Including Regions of Surge and Stall for Control Applications. NACA RM E54H24, 1954.

2. Novik, David, Heppler, Herbert, and Stiglic, Paul M.: Experimental Investigation of a Surge Control on a Turbojet Engine. NACA RM E55H03, 1955.

3. Delio, G. J., and Stiglic, P. M.: Experimental Investigation of Control Signals and the Nature of Stall and Surge Behavior in a Turbojet Engine. NACA RM E54I15, 1954.

4. Heppler, Herbert, Stiglic, Paul M., and Novik, David: Analytical and Experimental Investigation of a Temperature-Schedule Acceleration Control for a Turbojet Engine. NACA RM E56C08.

5. Otto, Edward W., Gold, Harold, and Hiller, Kirby W.: Design and Performance of Throttle-Type Fuel Controls for Engine Dynamics Studies. NACA TN 3445, 1955.

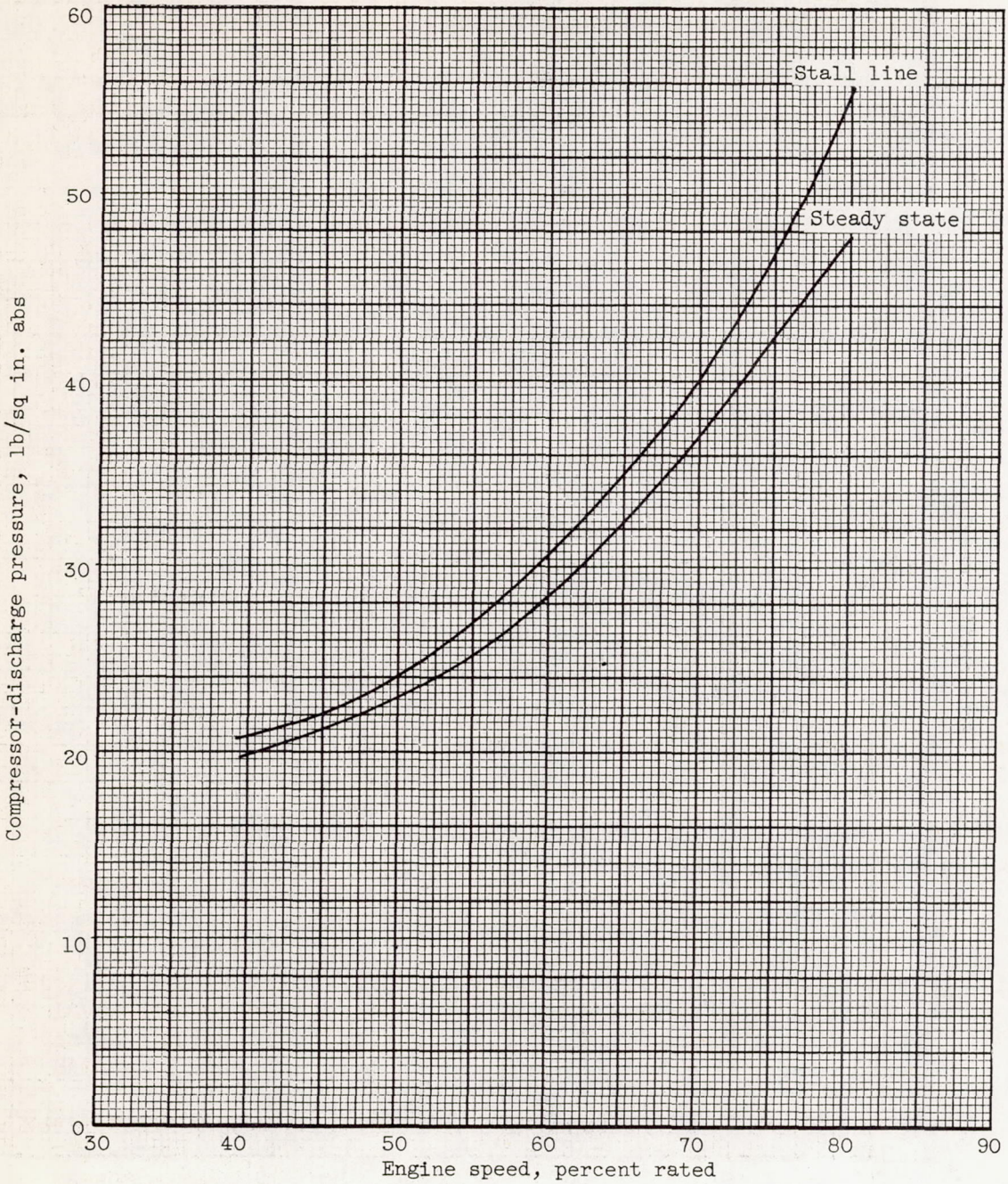

(a) Variation of compressor-discharge pressure with engine speed.

Figure 1. - Operating margin of a turbojet engine in terms of compressor-discharge pressure and acceleration at sea level.

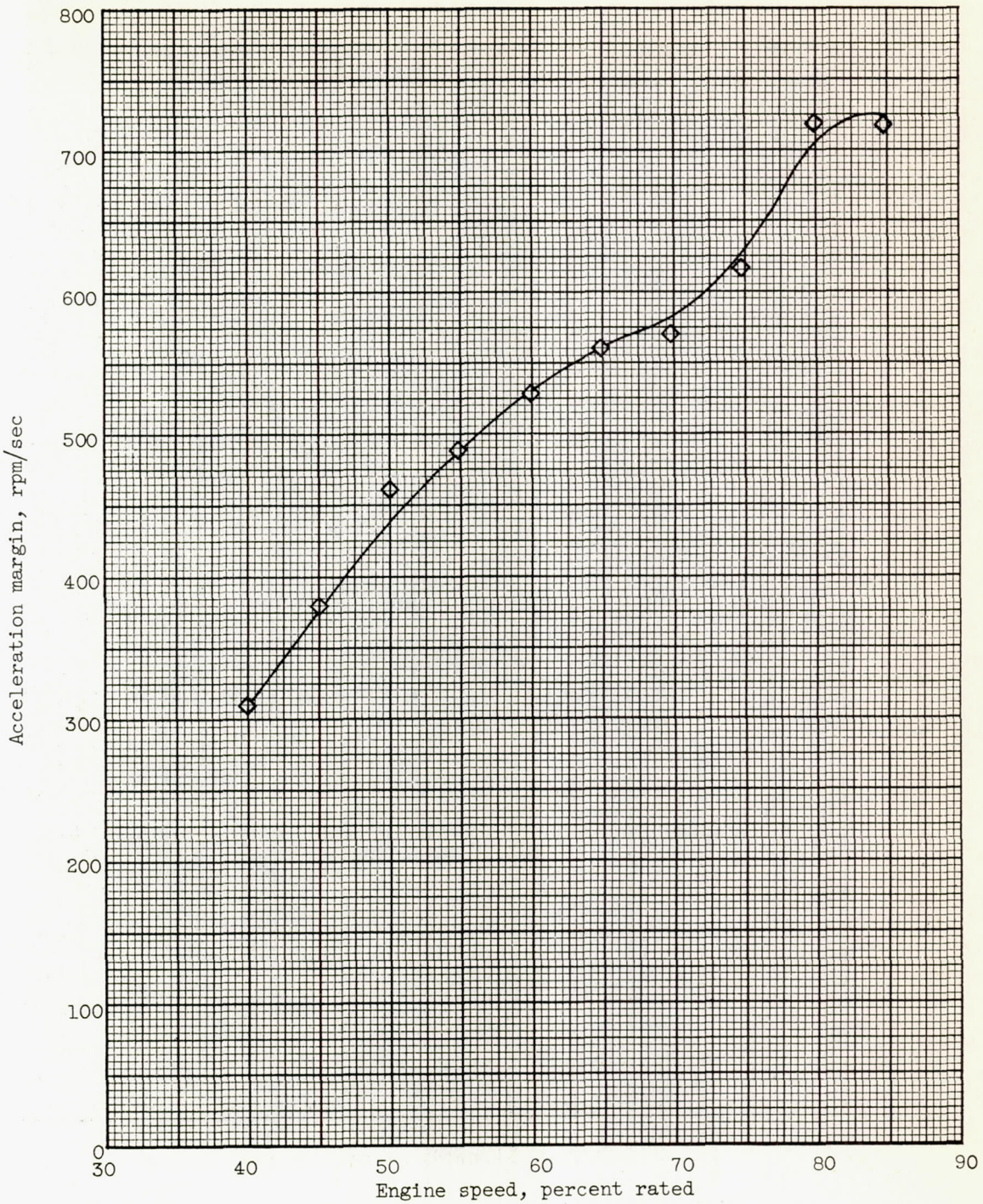

(b) Variation of engine acceleration margin with engine speed.

Figure 1. - Concluded. Operating margin of a turbojet engine in terms of compressor-discharge pressure and acceleration at sea level.

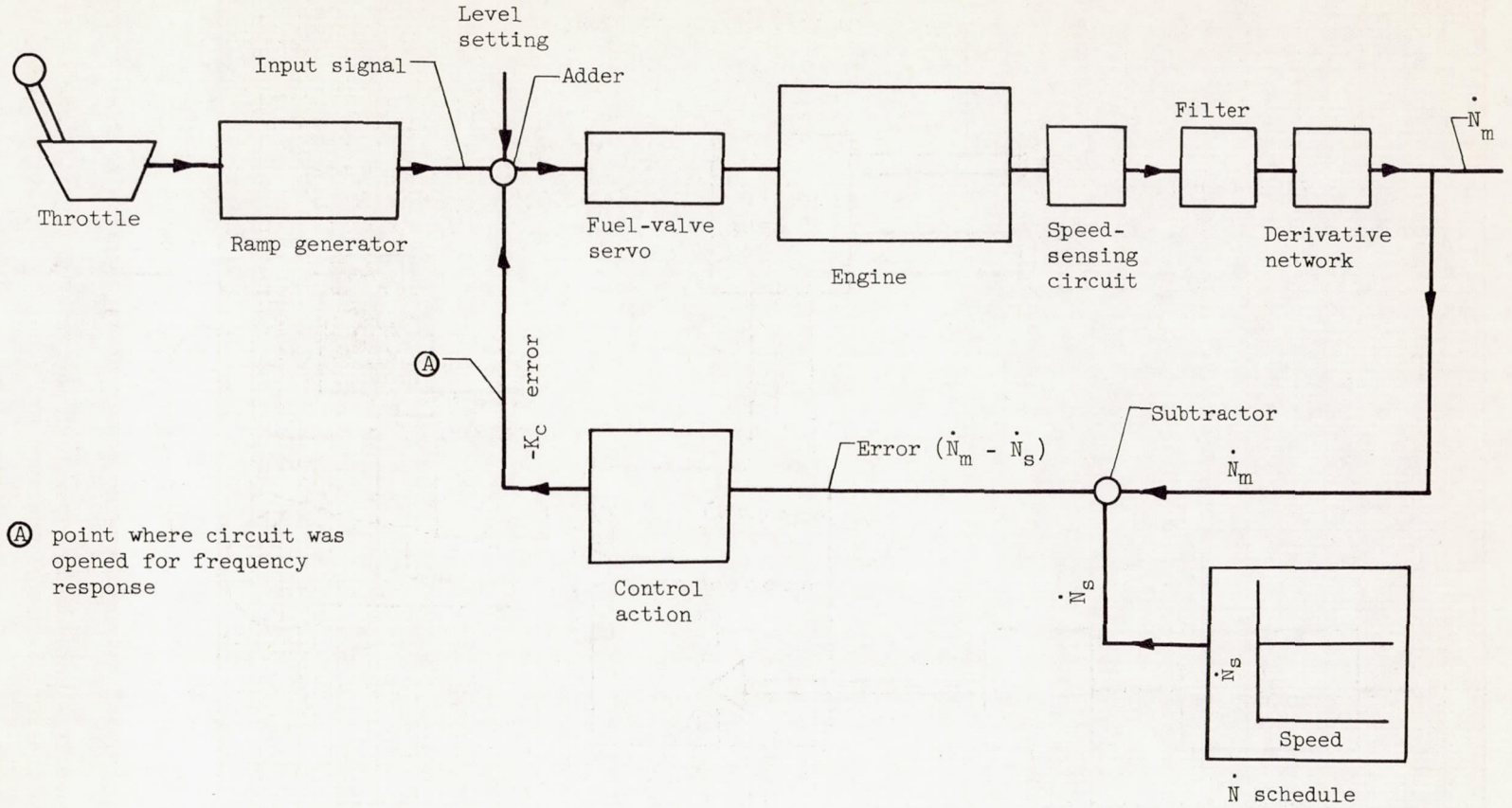

Figure 2. - Block diagram of control loop.

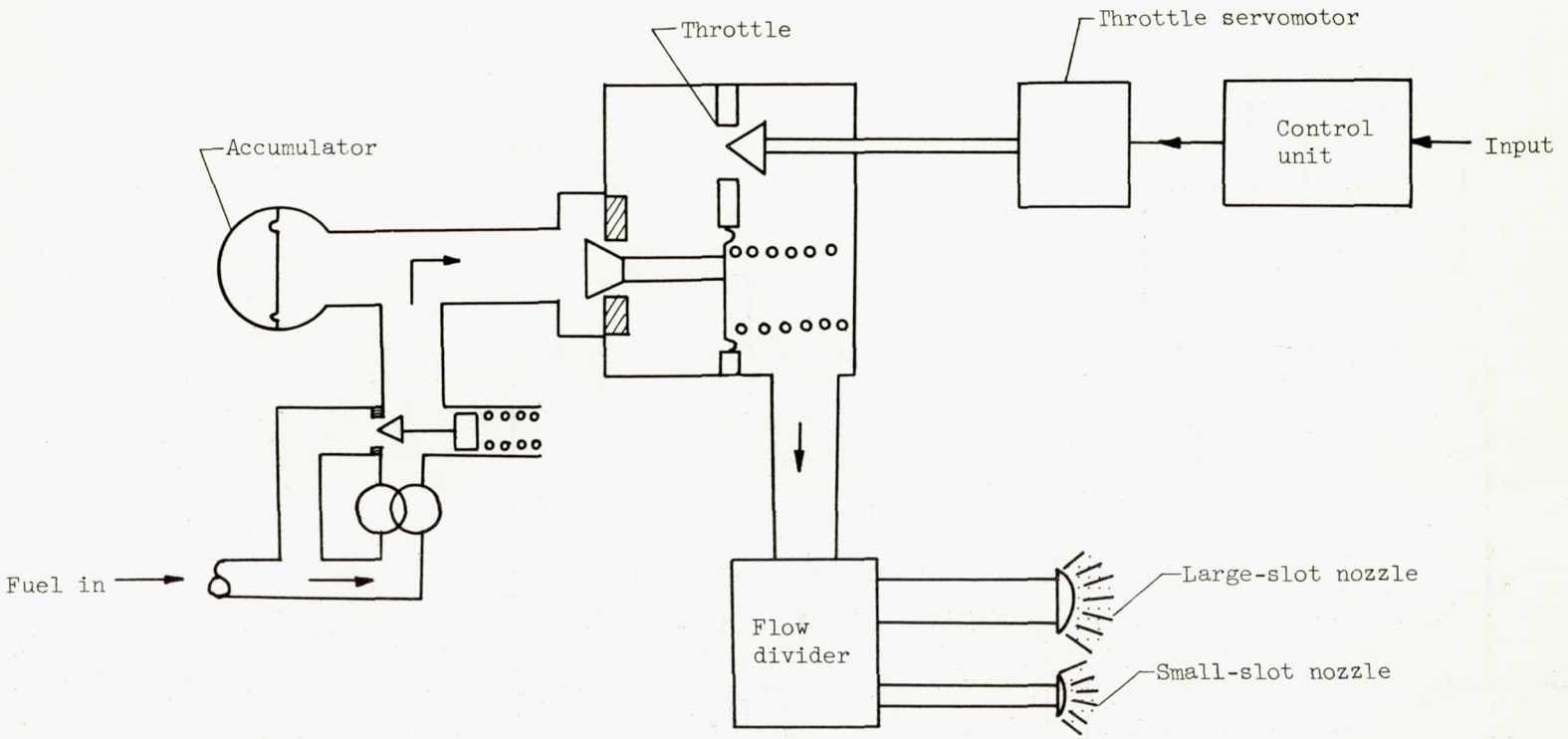

Figure 3. - Fuel system.

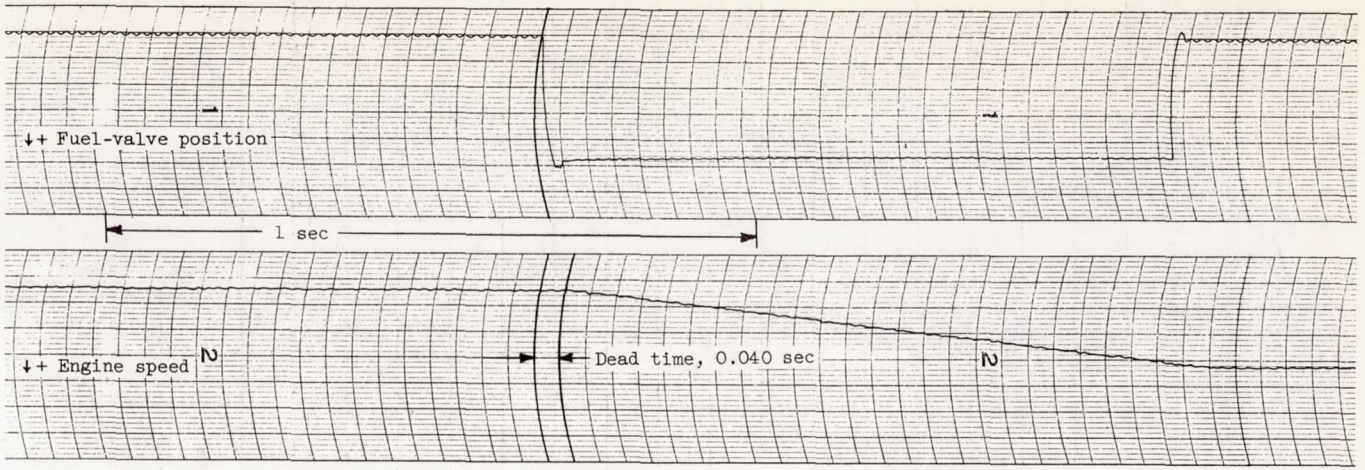

(a) From 73 percent rated speed.

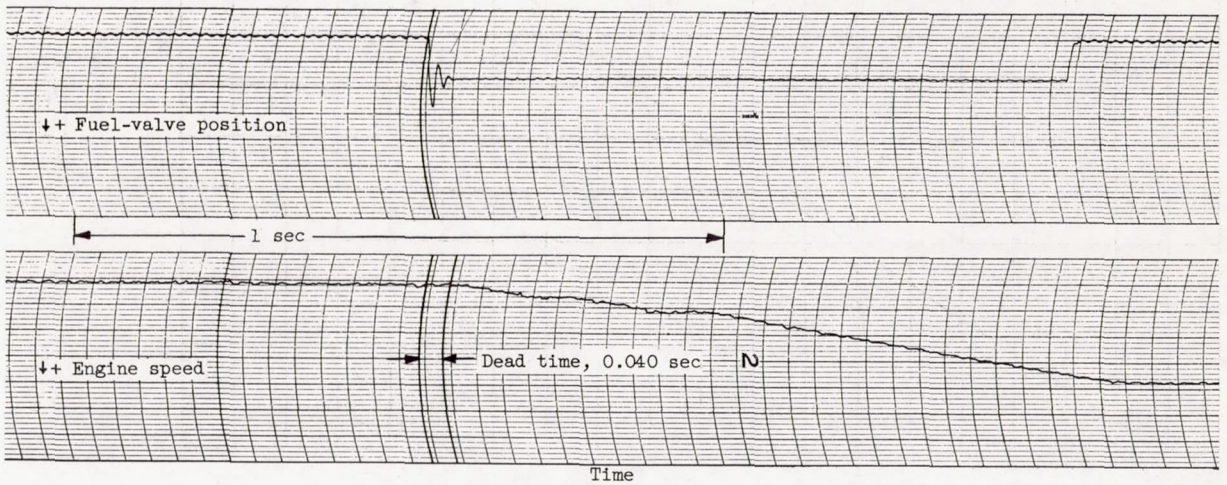

(b) From 62 percent rated speed.

Figure 4. - Step change in fuel flow showing dead time.

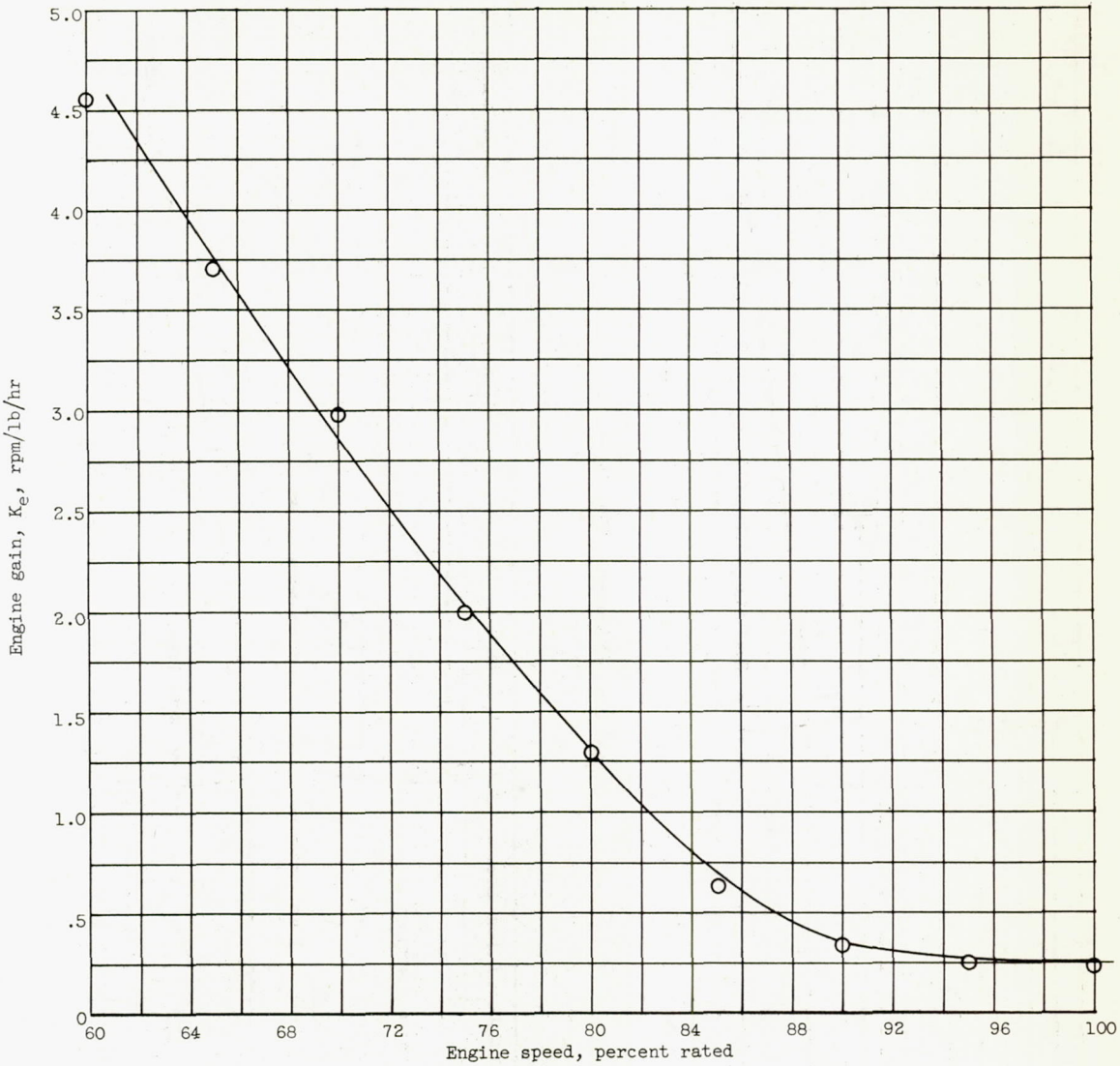

(a) Variation of engine gain with speed.

Figure 5. - Engine characteristics.

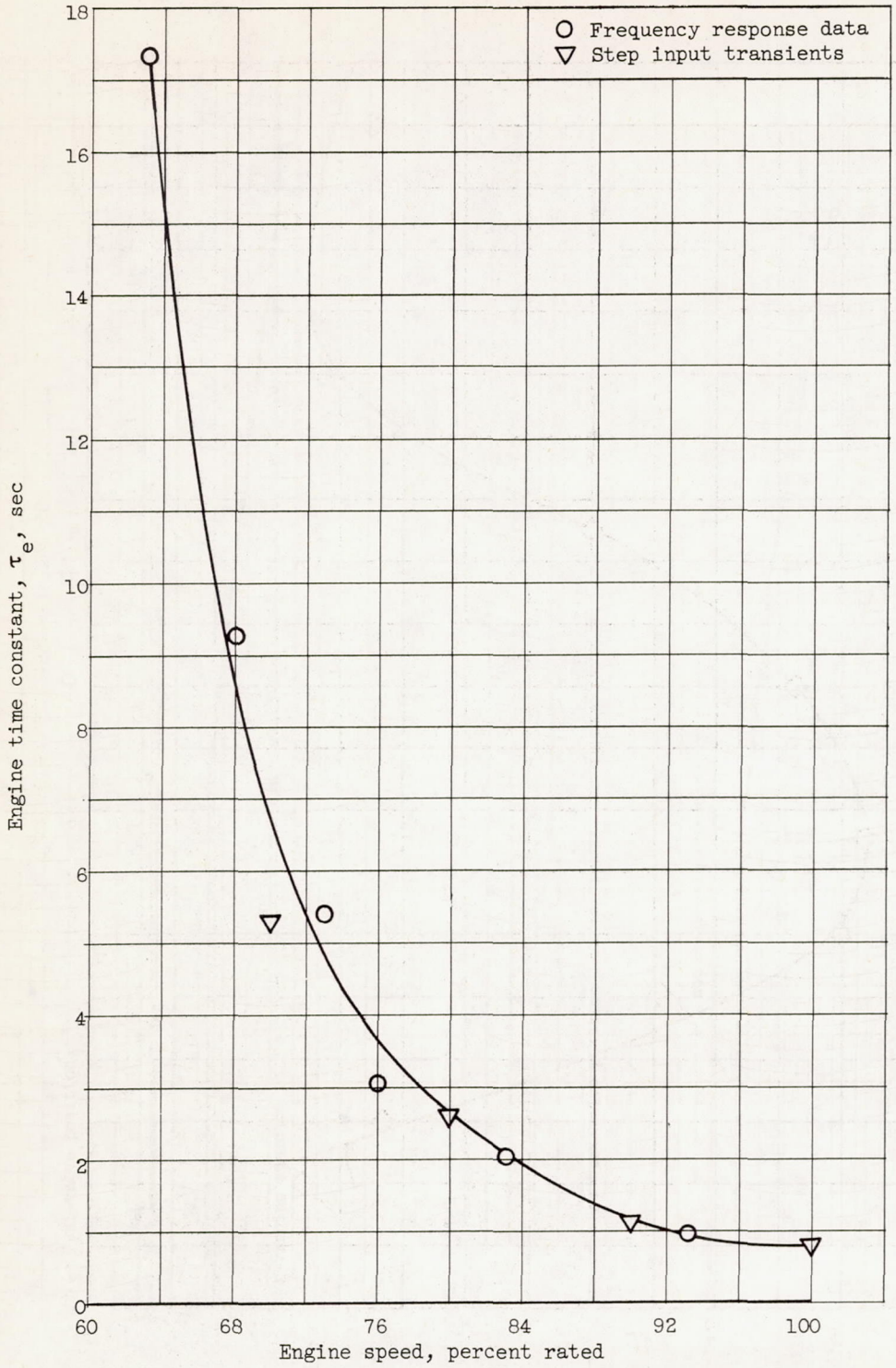

(b) Variation of engine time constant with engine speed.

Figure 5. - Continued. Engine characteristics.

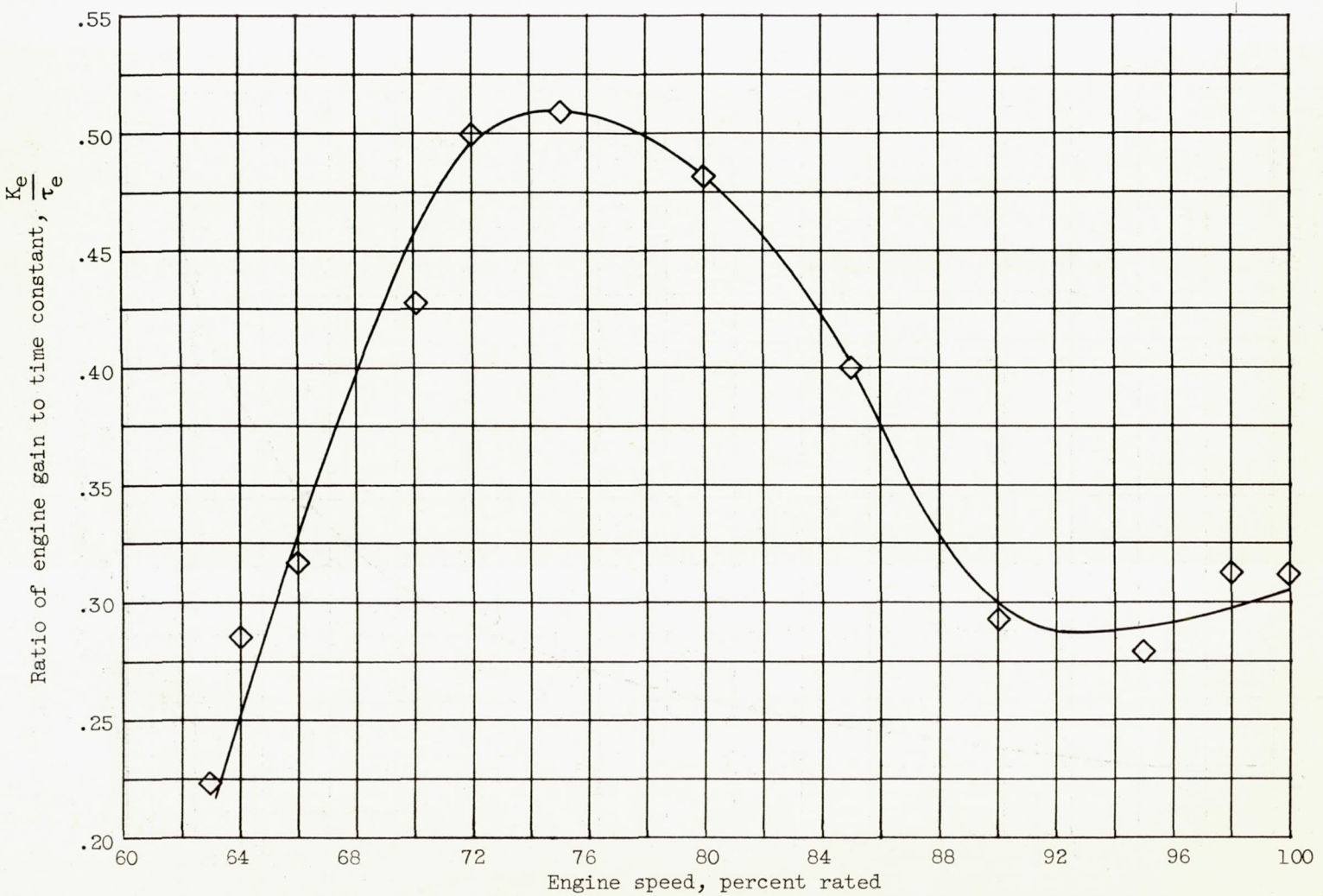

(c) Variation with engine speed of the ratio of engine gain to time constant.

Figure 5. - Concluded. Engine characteristics.

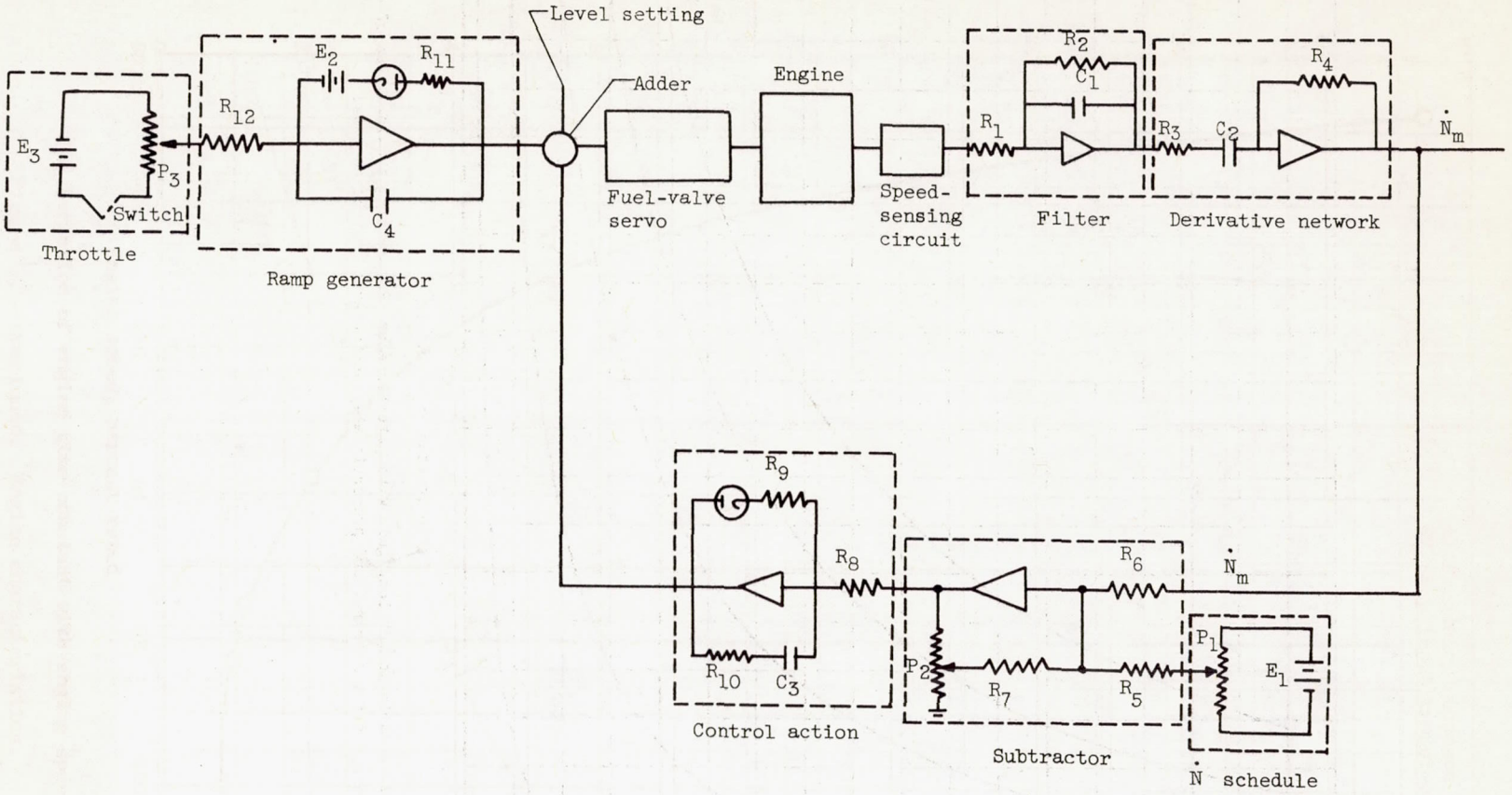

Figure 6. - Circuit diagram of control loop.

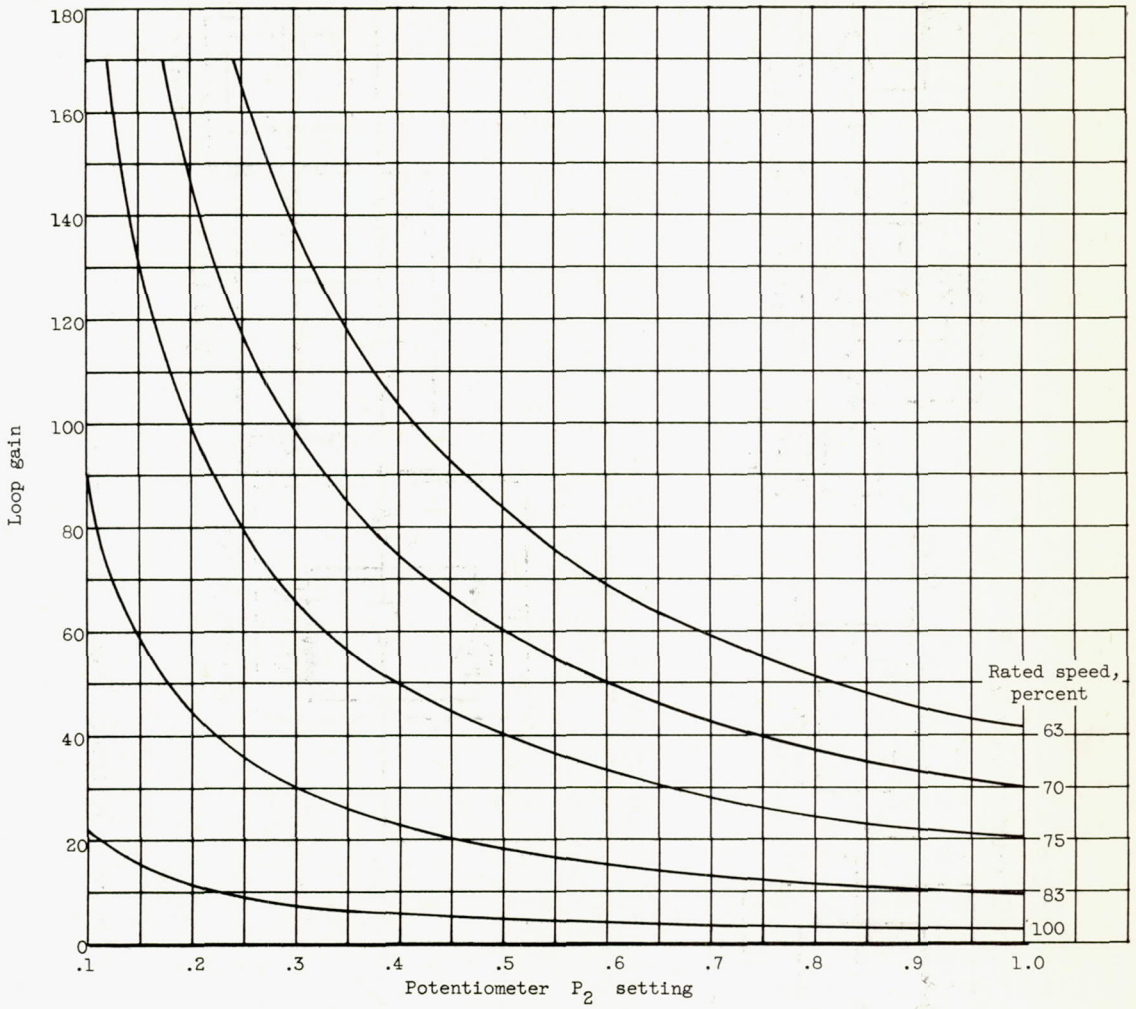

Figure 7. - Variation of loop gain with potentiometer P_2 setting showing lines of constant engine speed for integral and proportional-plus-integral control actions.

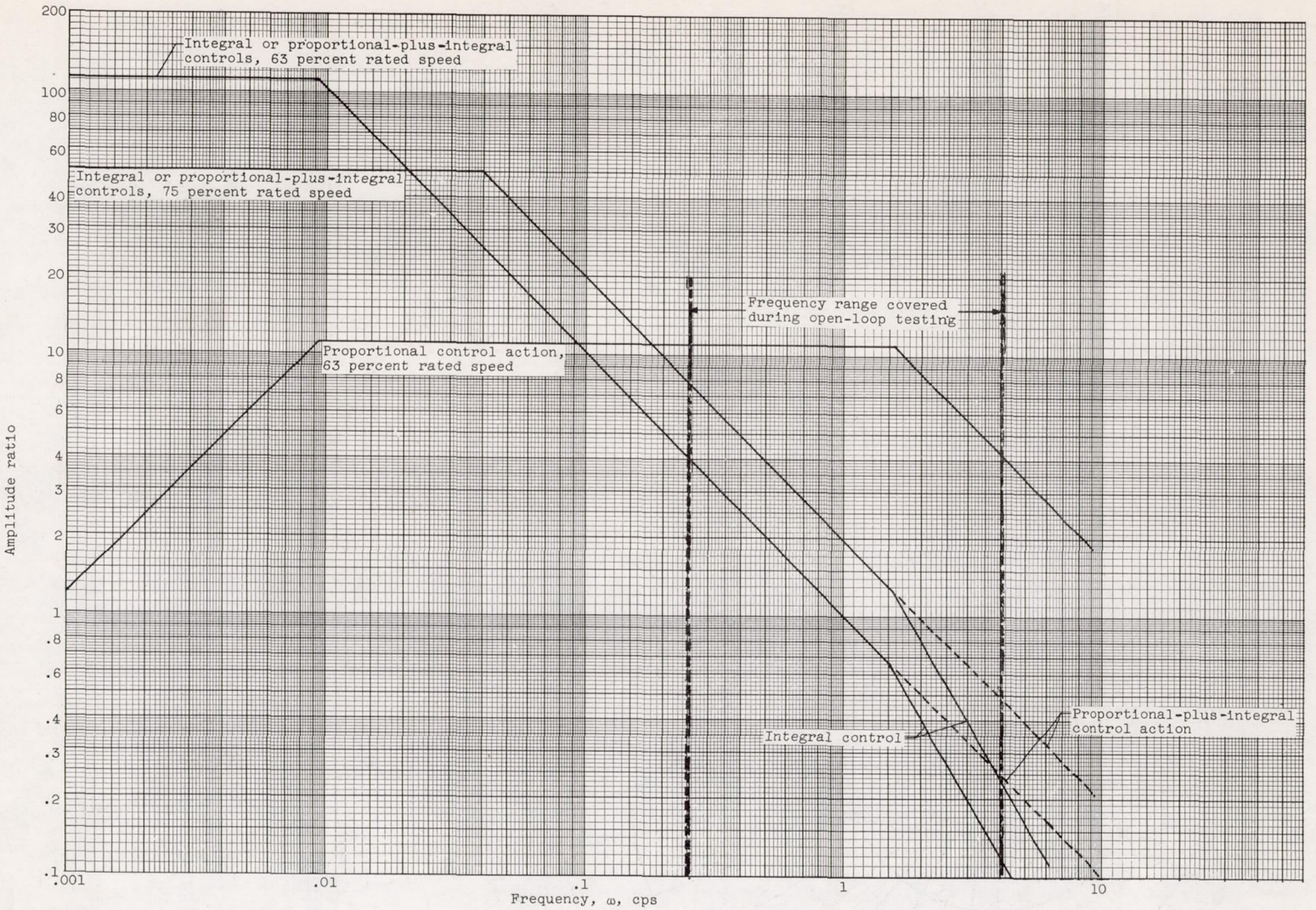

Figure 8. - Analytical open-loop frequency response at 63 and 75 percent rated speeds. Potentiometer P_2 setting, 0.4; proportional gain, 0.4; integrator time constant, 0.25.

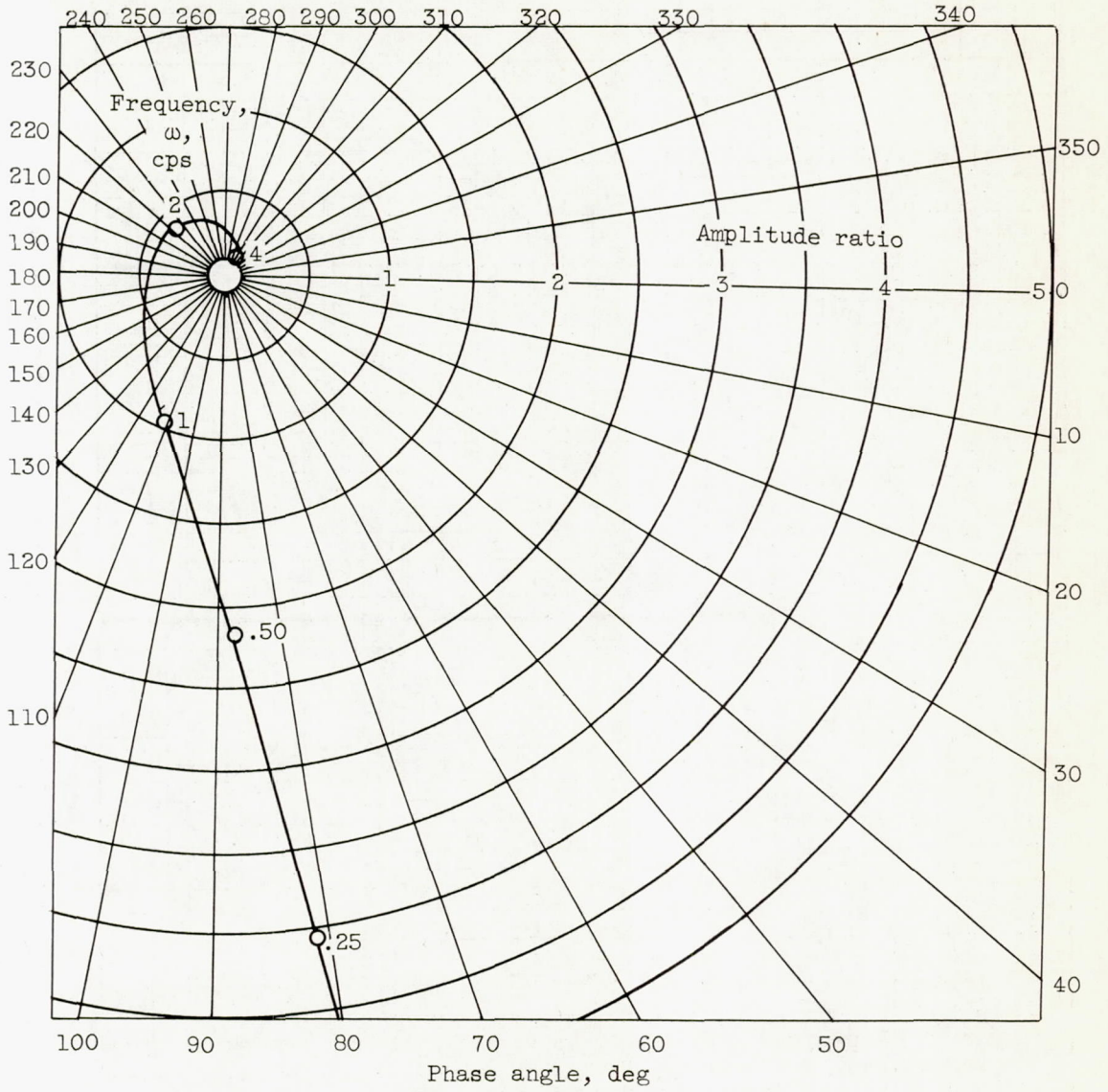

(a) Integral control action at 63 percent rated speed.

Figure 9. - Open-loop characteristics of control system. Potentiometer P_2 setting, 0.4.

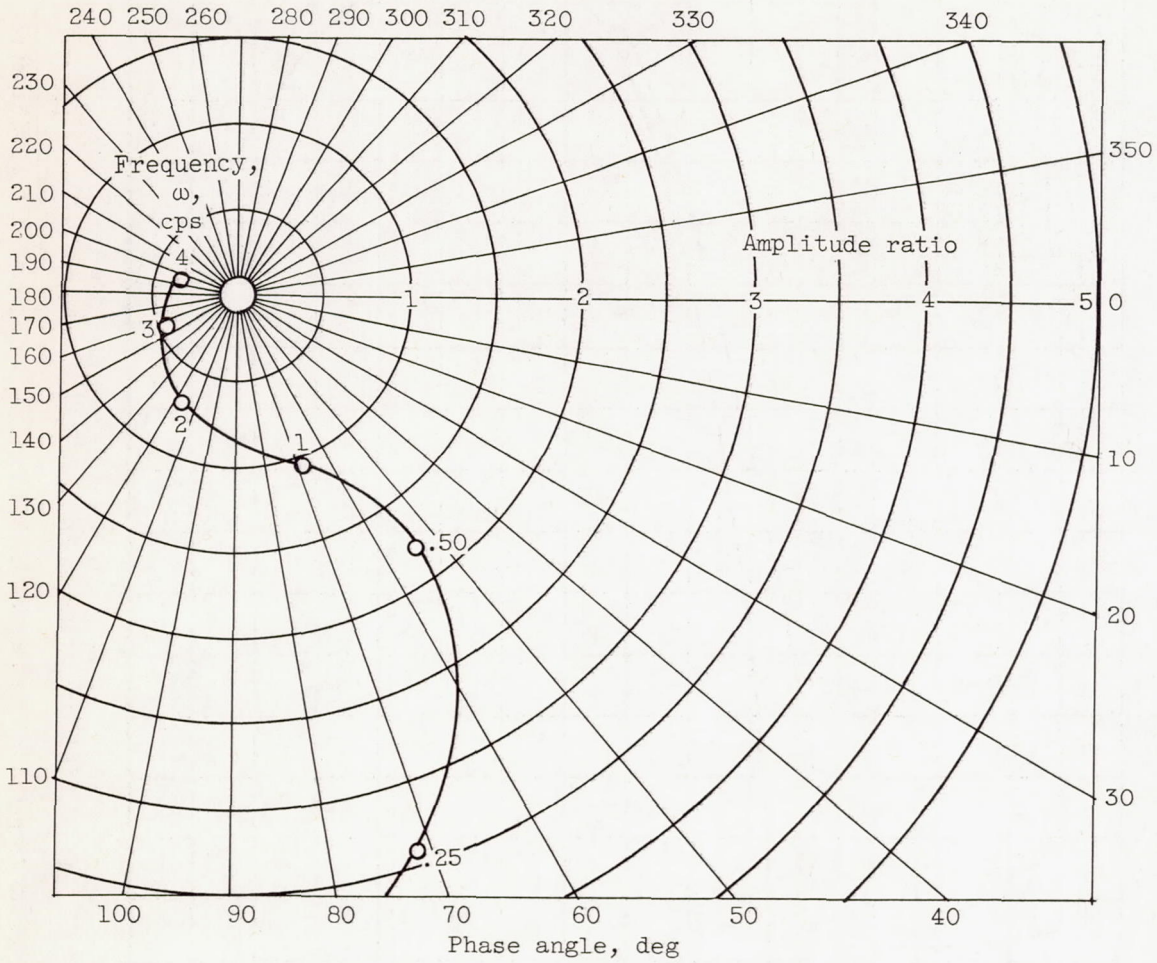

(b) Proportional-plus-integral control action at 63 percent rated speed.

Figure 9. - Concluded. Open-loop characteristics of control system. Potentiometer P_2 setting, 0.4.

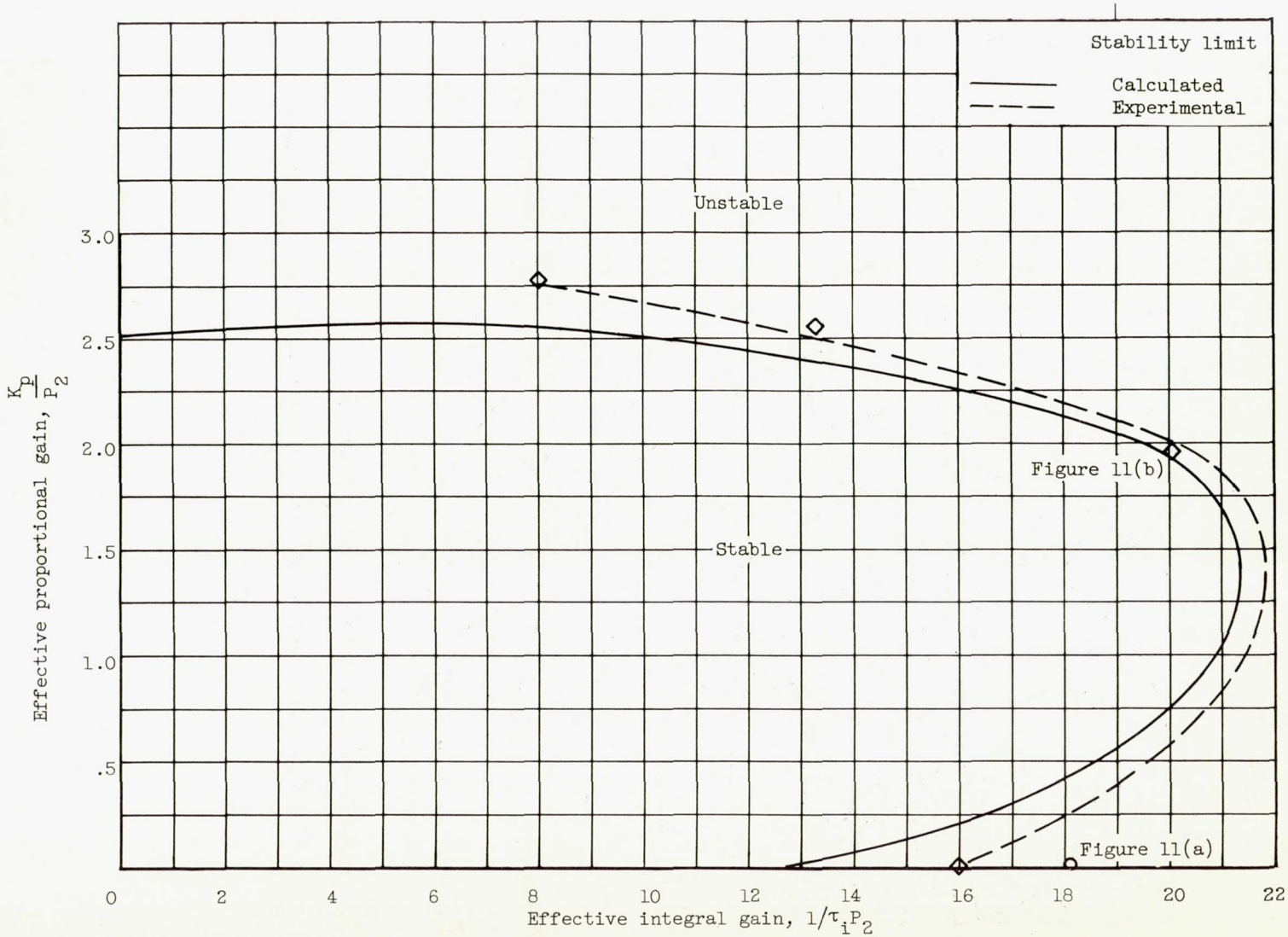

Figure 10. - Stability limit at 75 percent rated speed of proportional, proportional plus integral and integral control systems.

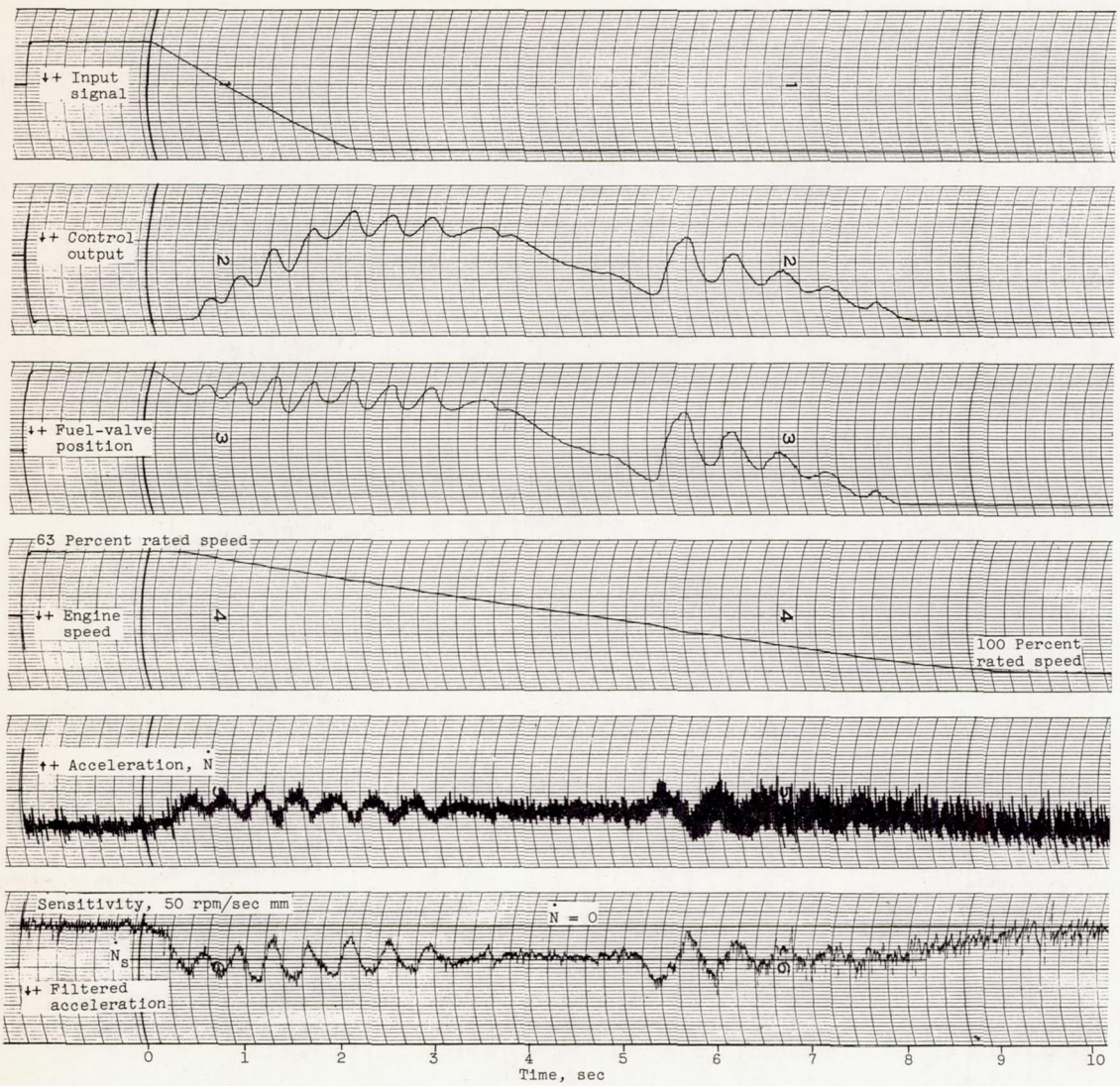

(a) Integral control action beyond stability limit. Effective integral gain, 18.2.

Figure 11. - Controlled engine transients.

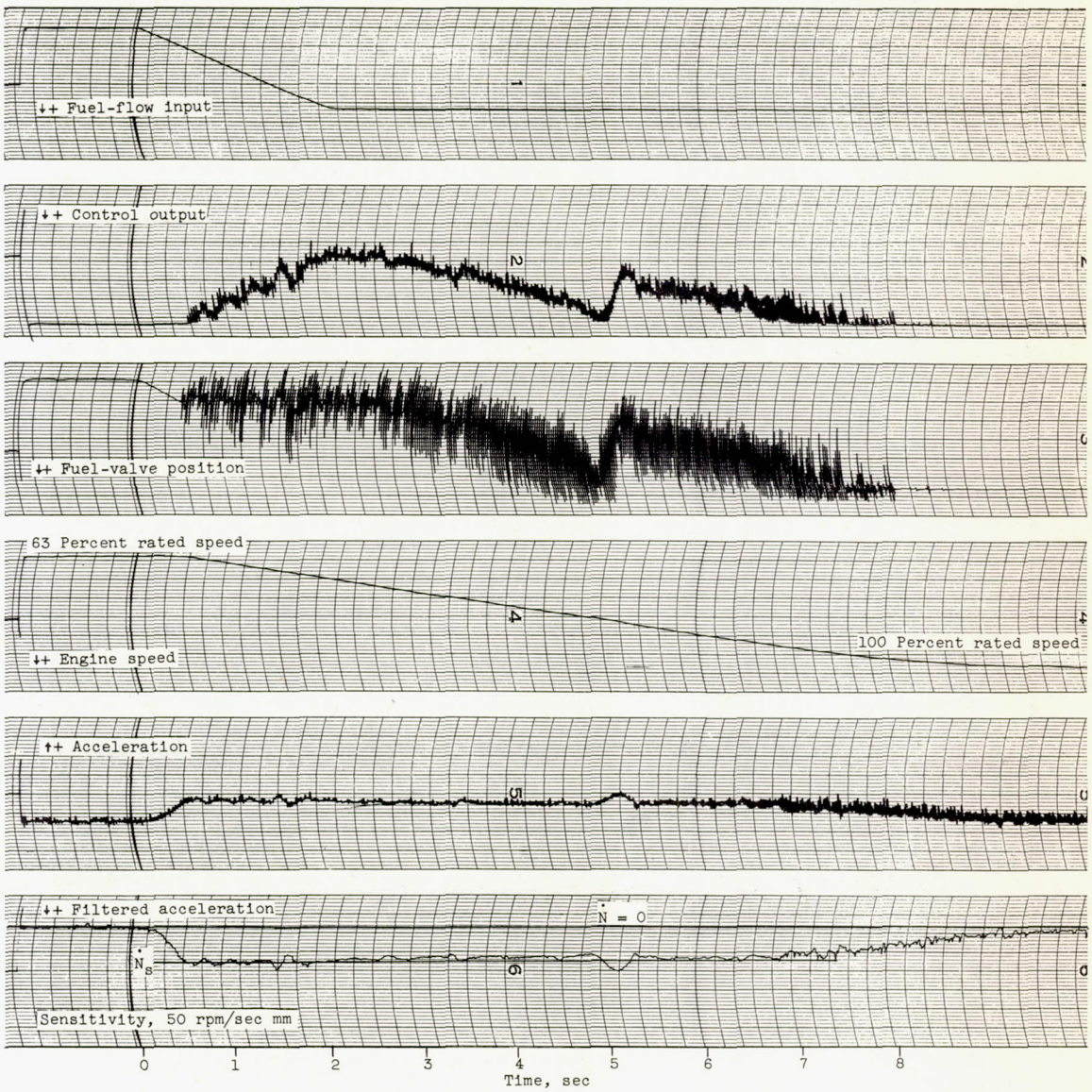

(b) Proportional-plus-integral control action near stability limit. Effective integral gain, 20; effective proportional gain, 2.0.

Figure 11. - Concluded. Controlled engine transients.

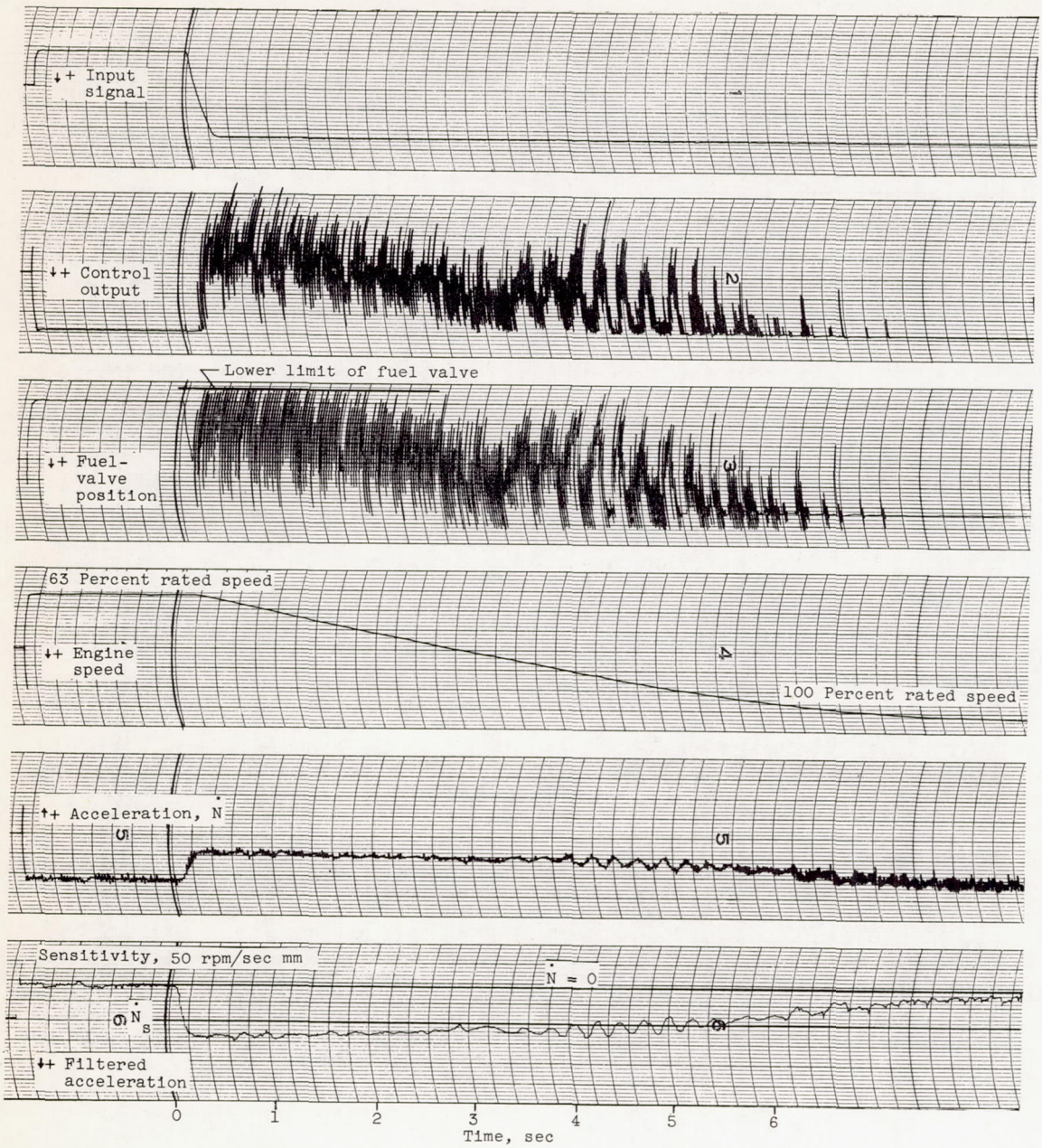

Figure 12. - Unstable run of proportional control action. Proportional gain, 3.0; potentiometer P_2 setting, 0.4.

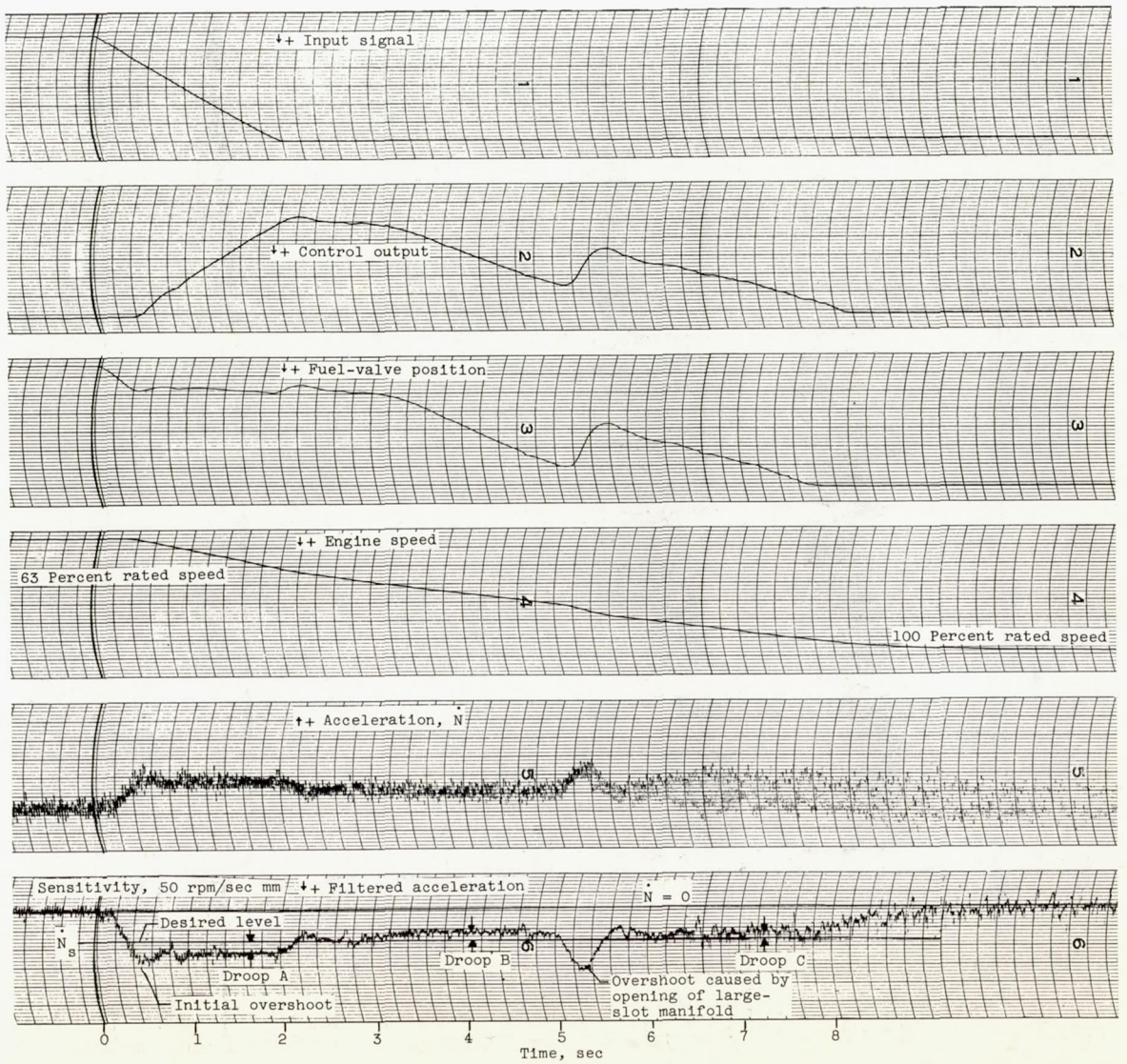

Figure 13. - Typical transient showing various droops and overshoots. Potentiometer P_2 setting, 0.6.

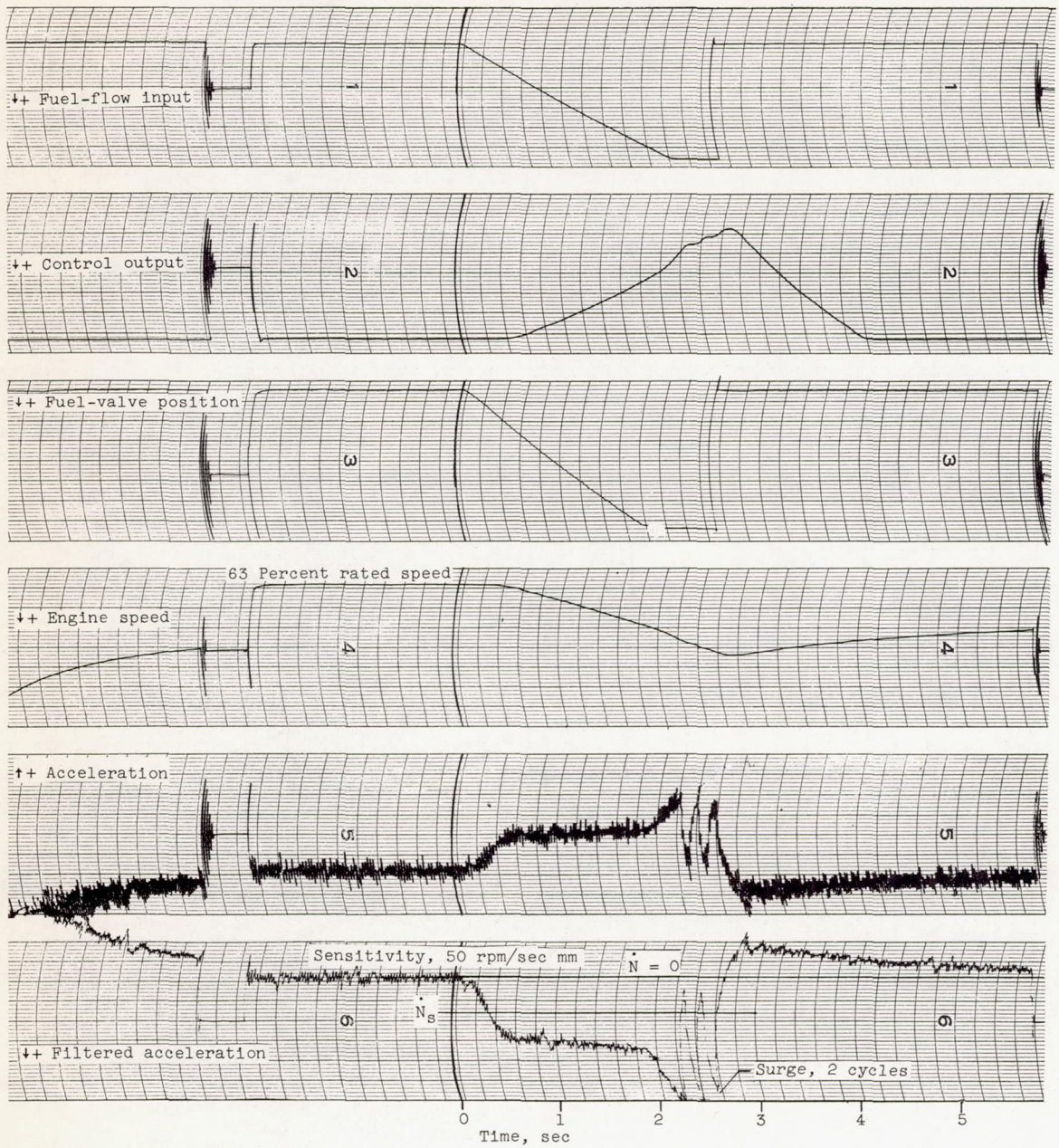

(a) Uncontrolled engine.

Figure 14. - Typical transients.

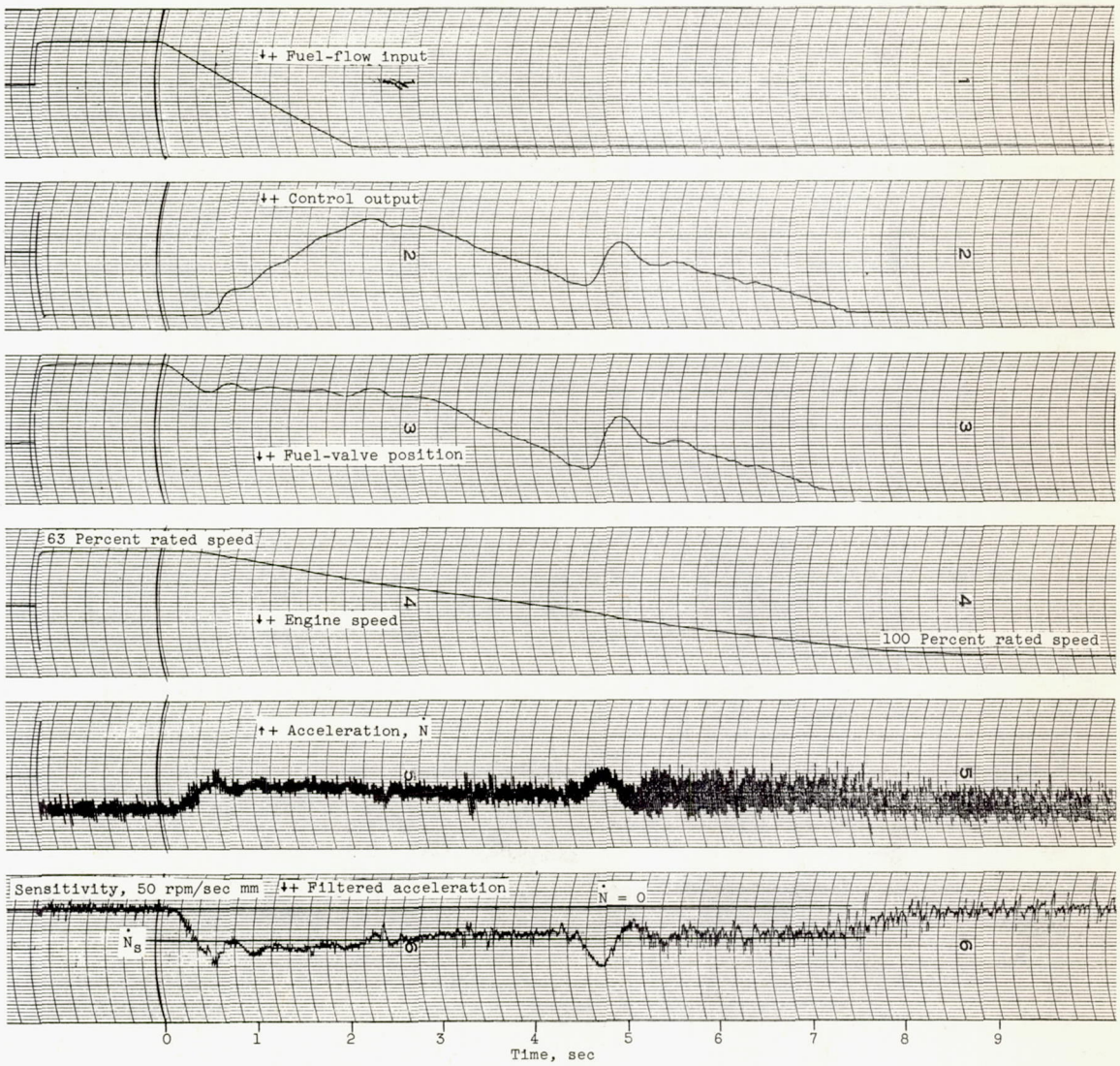

(b) Integral control action. Potentiometer P_2 setting, 0.4.

Figure 14. - Continued. Typical transients.

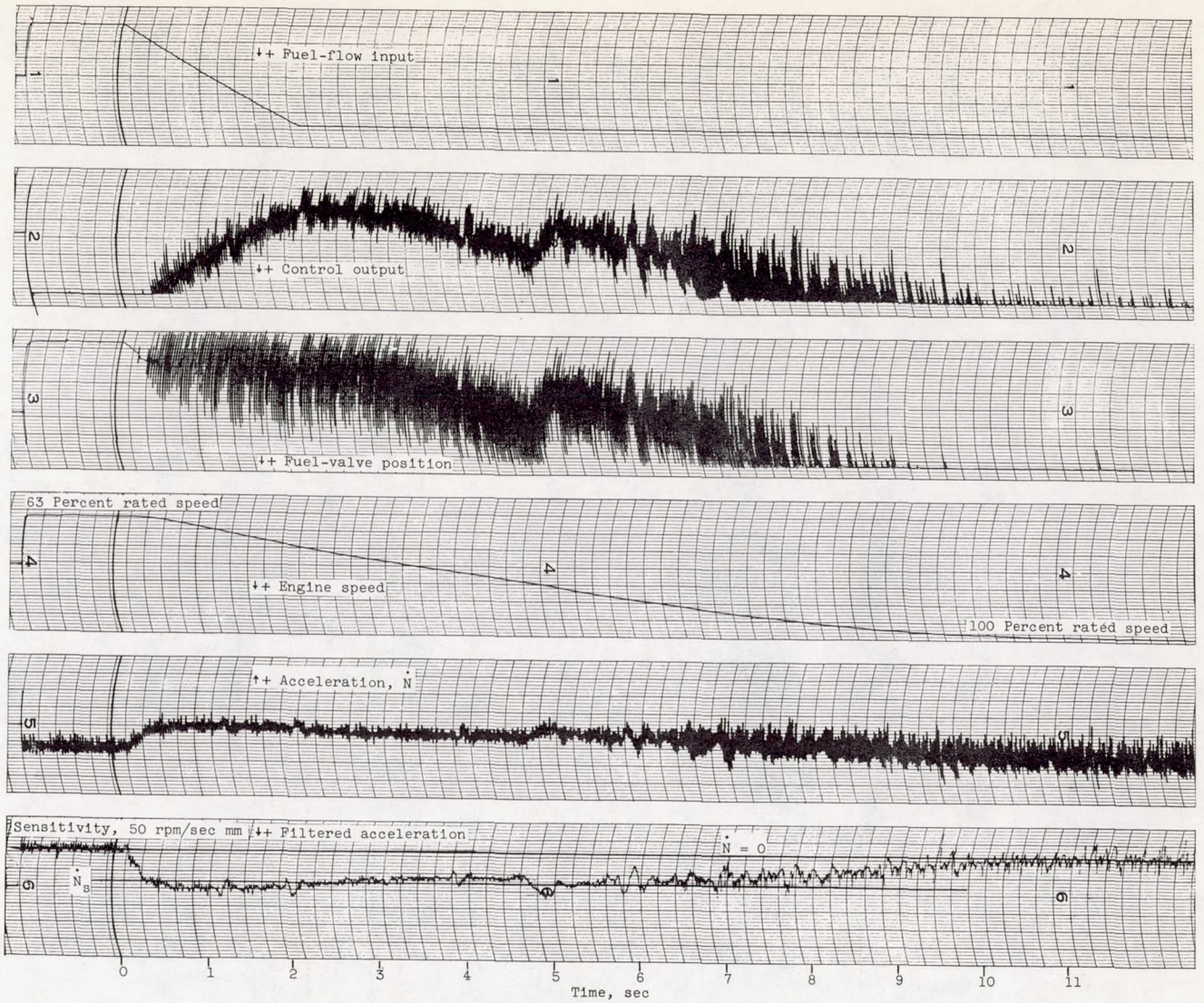

(c) Proportional-plus-integral control action.

Figure 14. - Continued. Typical transients.

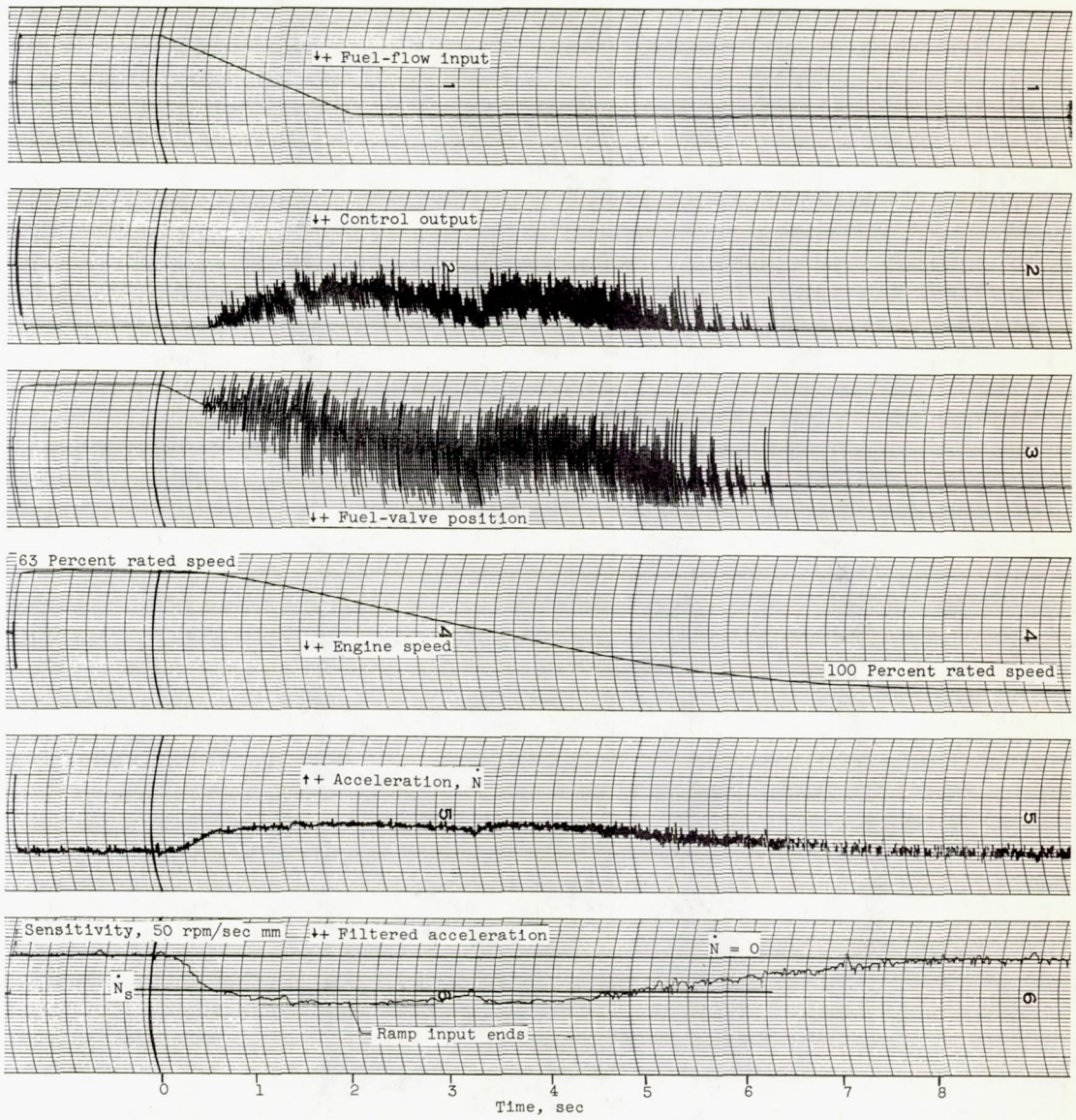

(d) Proportional control action.

Figure 14. - Concluded. Typical transients.

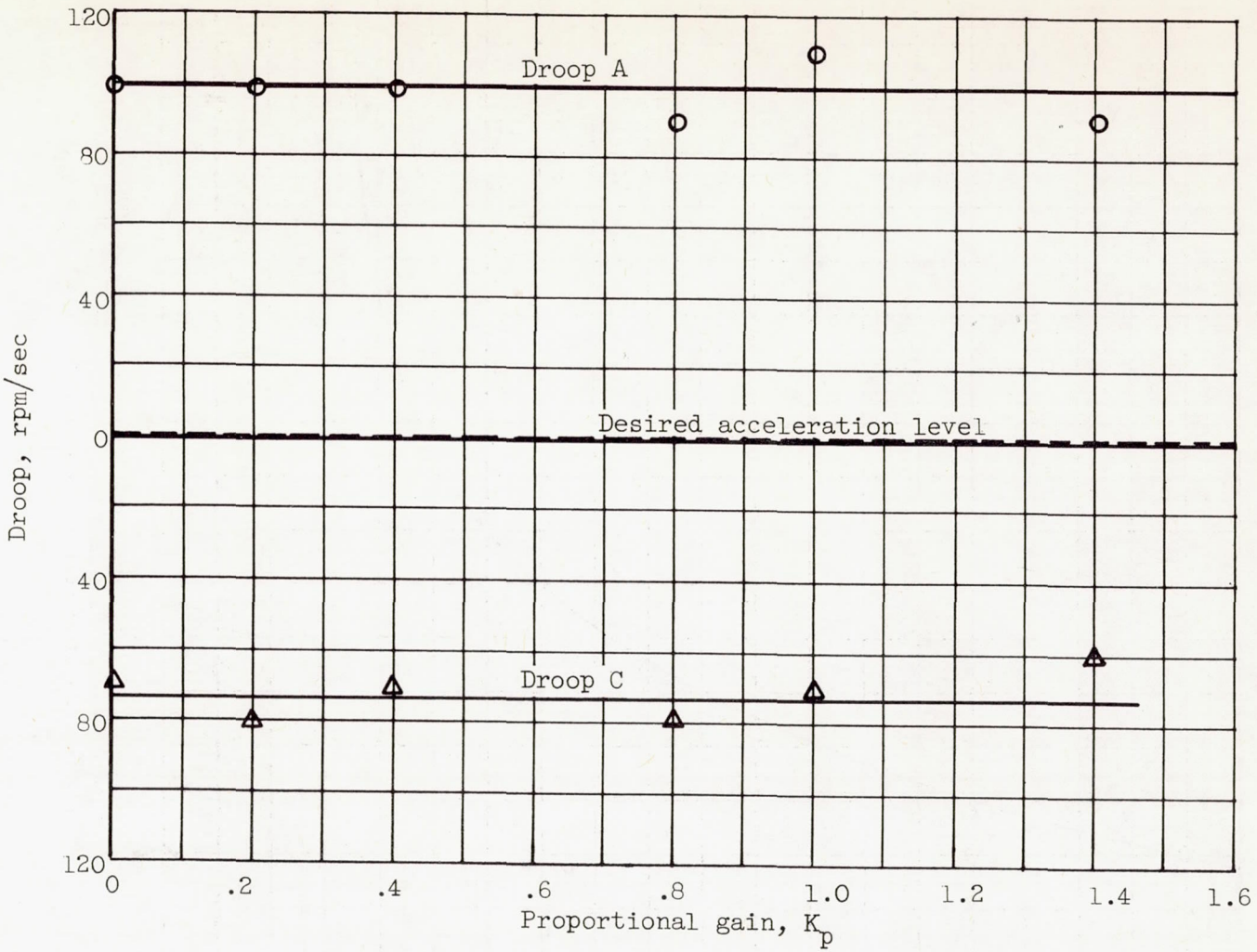

Figure 15. - Variation of droop with proportional gain for proportional-plus-integral control action. Potentiometer P_2 setting, 0.5.

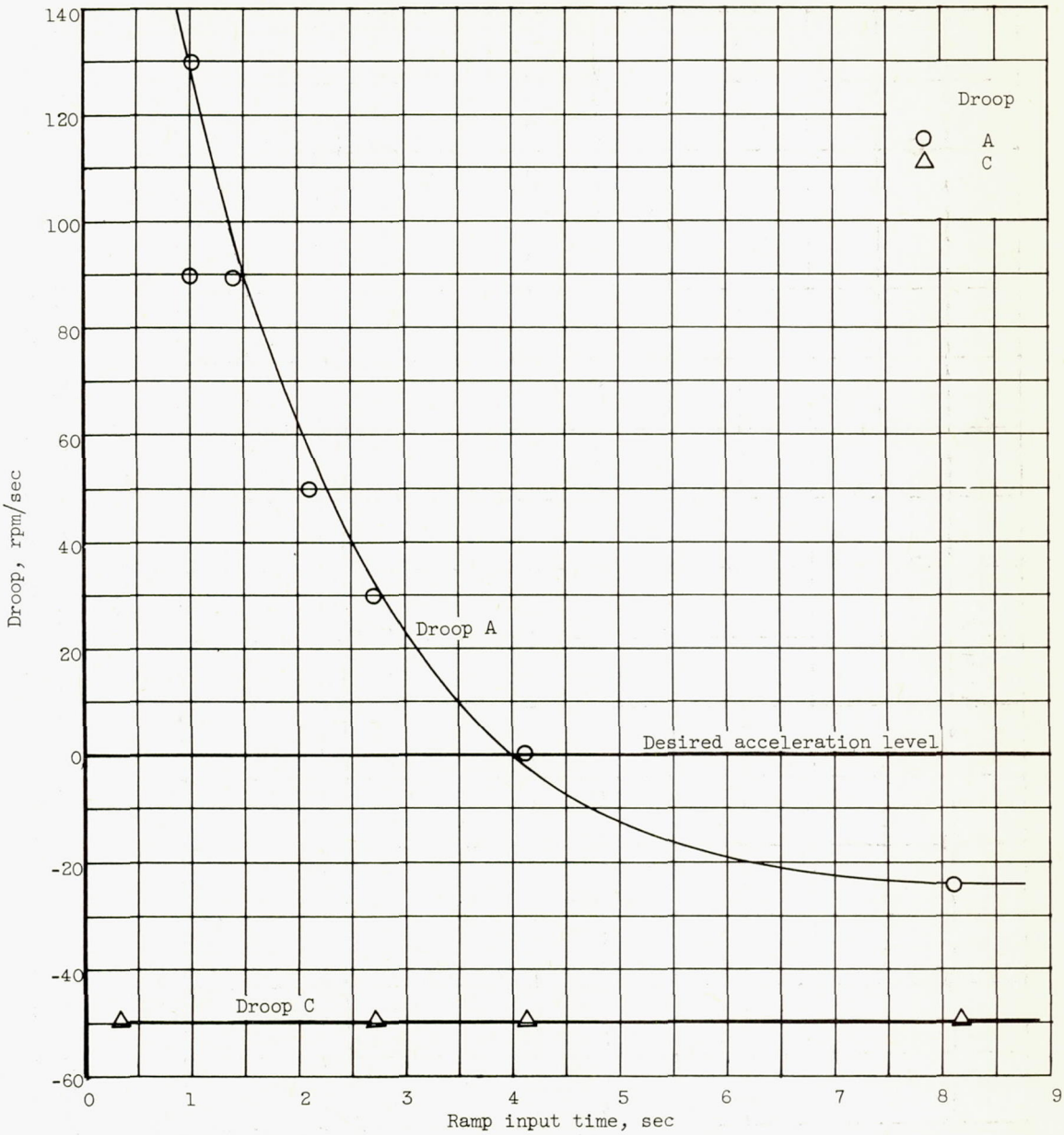

Figure 16. - Effect of rate of ramp input signal on droop.

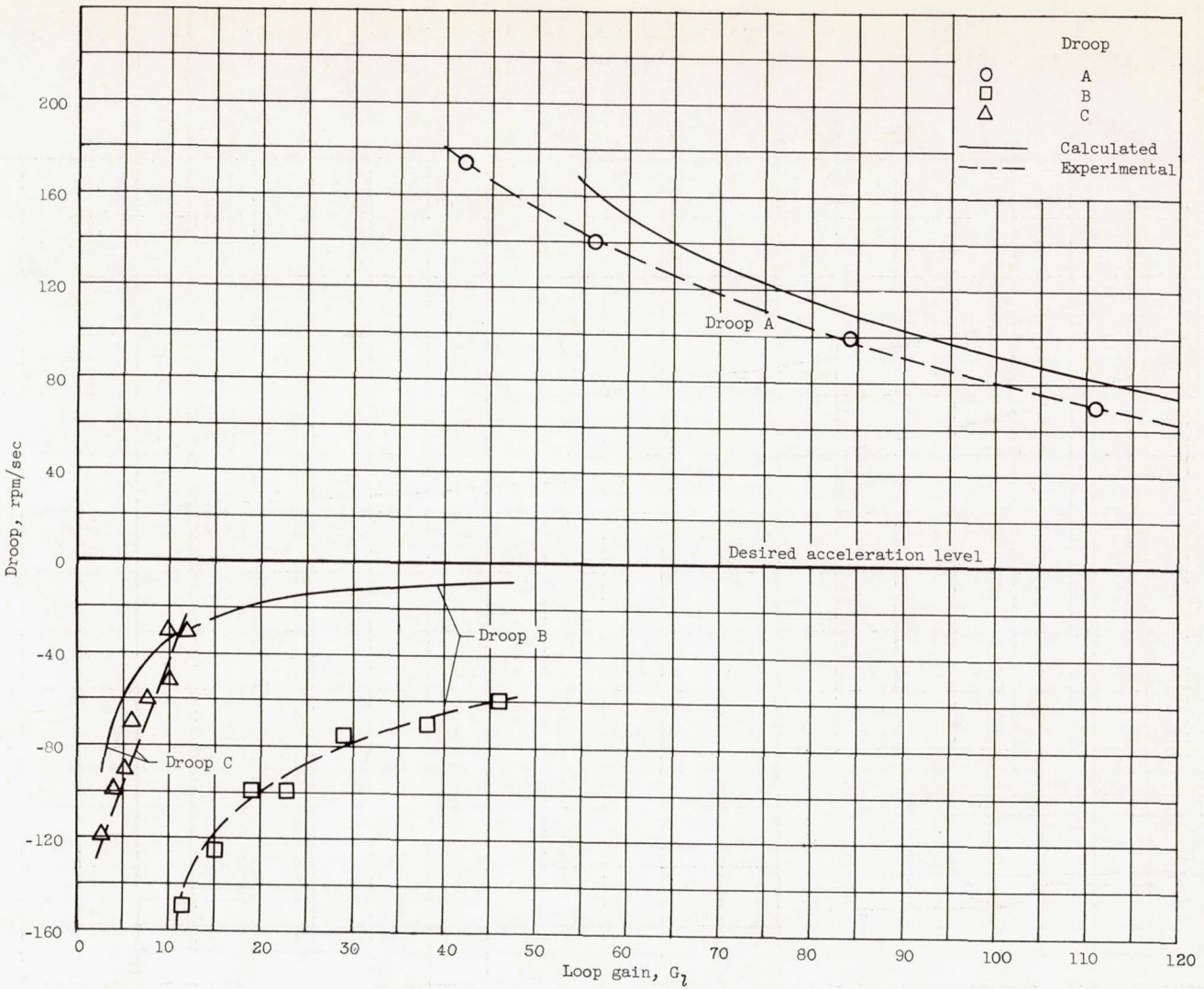

Figure 17. - Effect of loop gain on droop for integral and proportional-plus-integral control actions for 2-second ramp input signal.

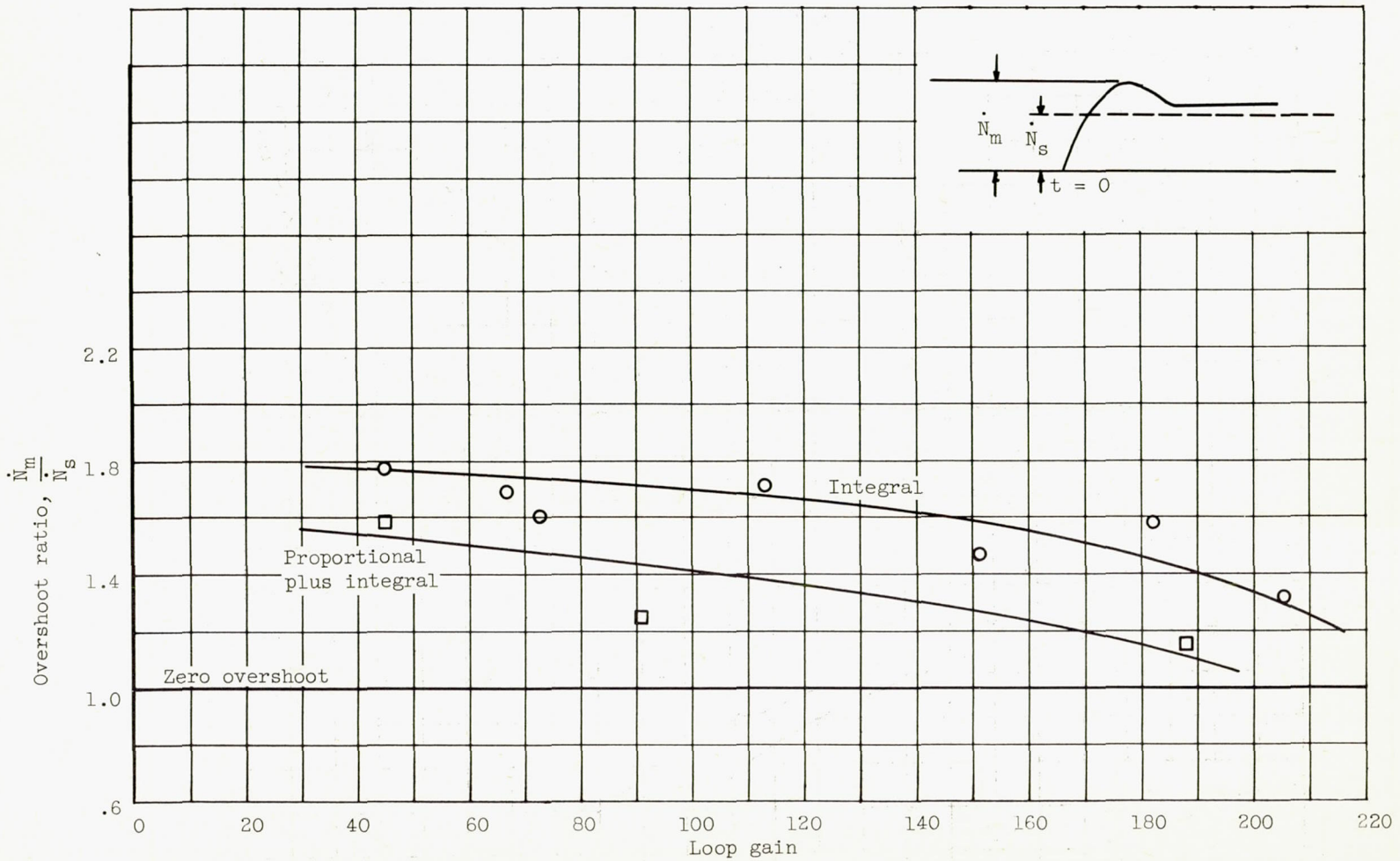

Figure 18. - Effect of loop gain on overshoot for integral and proportional-plus-integral control action. Input signal ramp, 2 seconds; potentiometer P_2 setting, 0.4.

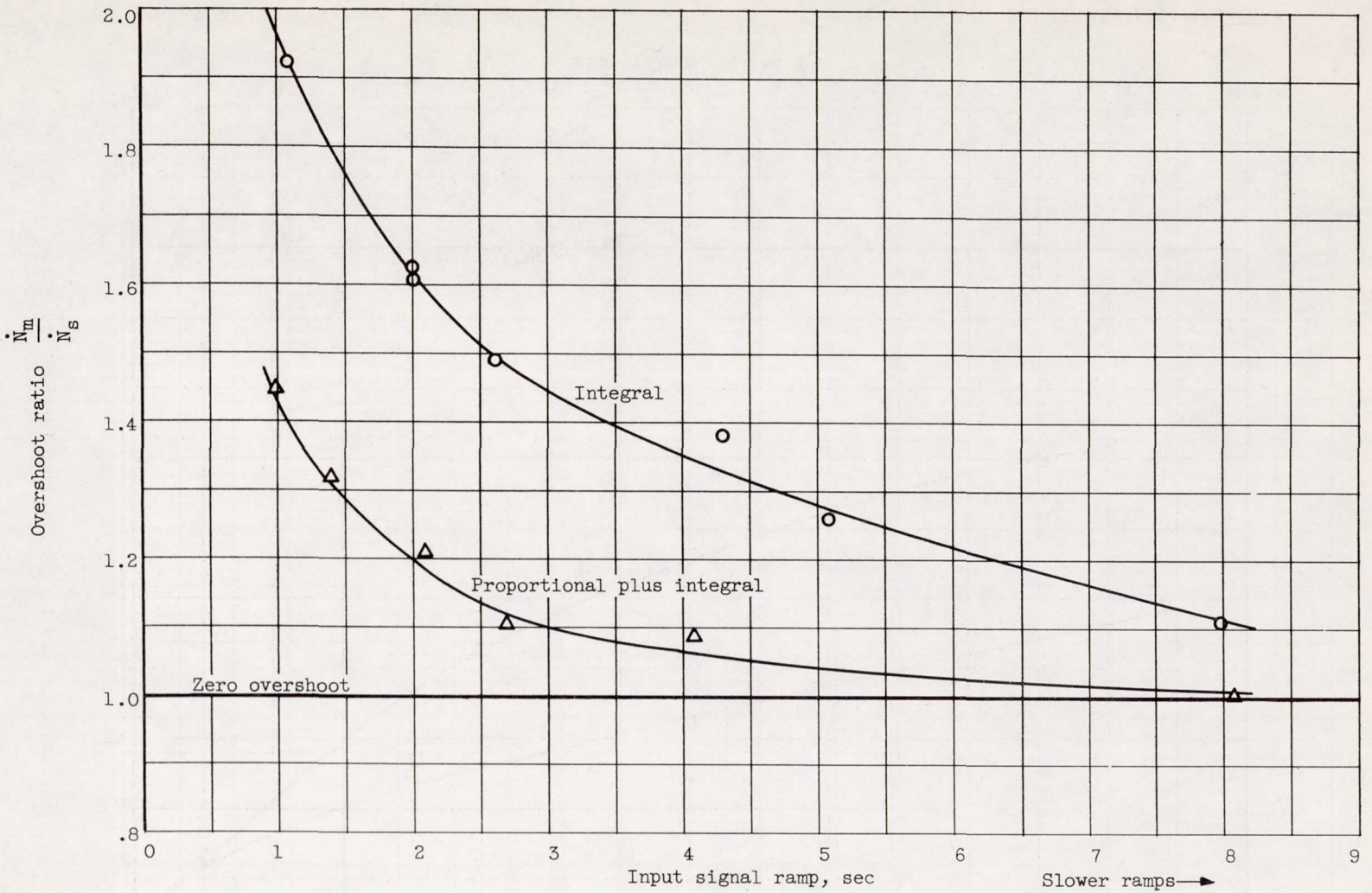

Figure 19. - Effect of rate of ramp input on overshoot for integral and proportional-plus-integral control actions.

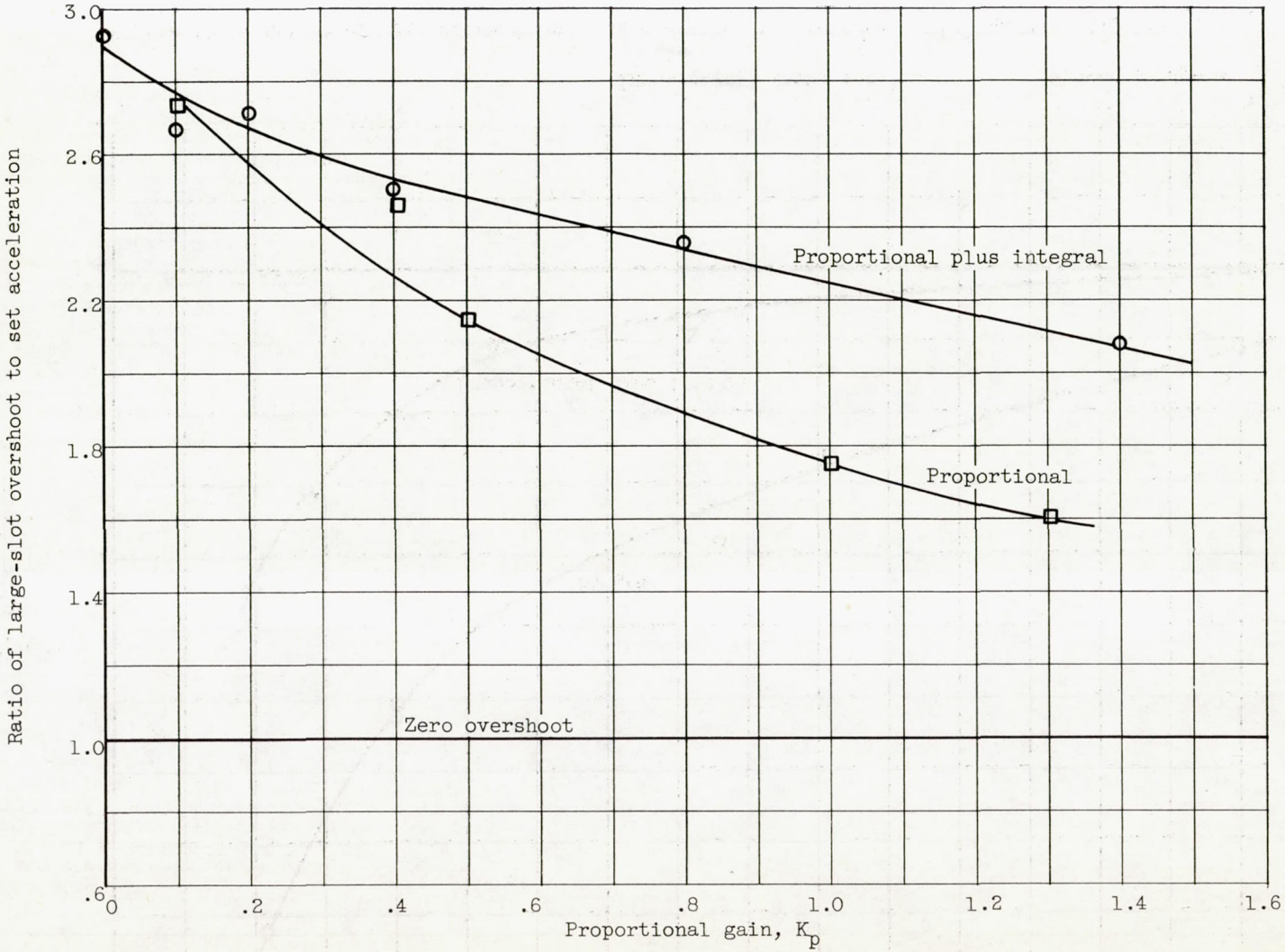

Figure 20. - Effect of proportional gain on overshoot. Input signal ramp, 2 seconds; potentiometer P_2 setting, 0.4.

NACA - Langley Field, Va.